# Co-release of opposing signaling molecules from cortical neurons controls the escalation and release of aggression

Rachel E. Gatlin[1], Jordyn Gagon[1], Sewon Park[1], Damhyeon Kwak[2], Hailee Walker[2], Lo Kronheim[1], Thomas Everett[1], Ashley Covington[1], Michaela M. Fluck[1], Tobias Zickmund[1], Nicholas A. Frost[2], Moriel Zelikowsky[1]*

1. Department of Neurobiology, University of Utah, School of Medicine, Salt Lake City, UT, 84112.

2. Department of Neurology, University of Utah, School of Medicine, Salt Lake City, UT, 84132.

* Corresponding Author: Moriel Zelikowsky, moriel.zelikowsky@neuro.utah.edu

**SUMMARY**

Prolonged social isolation induces a distinct state characterized by numerous impacts on behavior, including increased aggression and altered social behaviors, but the contributions of cortical circuits to these behaviors are poorly understood. Here, we find that social isolation promotes aggression and increases investigatory behaviors leading up to aggression in both males and female mice. Genetic characterization of the neuropeptidergic population of Tachykinin-2 expressing ($Tac2^+$) neurons in the medial prefrontal cortex (mPFC) reveals a population of predominately early-layer GABAergic neurons that are activated by aggressive encounters in isolated mice. Cells expressing the Neurokinin 3 receptor, which binds the peptide product of *Tac2*, are similarly activated by aggressive interactions in isolated mice. Loss of function perturbations targeting the co-release of Neurokinin B (NkB), the stimulatory peptide encoded by the gene Tac2, and the inhibitory neurotransmitter GABA from mPFC $Tac2^+$ neurons, reveals dissociable functions for each signaling molecule in the distinct behaviors that tile an aggressive encounter. GABA transmission form $Tac2^+$ neurons controls the release of aggression, whereas Tac2/NkB signaling controls the investigatory behaviors escalating to aggression. These findings reveal dissociable roles for opposing signaling molecules released from the same neuron in the control over aggression, suggesting a neurochemical mechanism by which internal states may exert coordinated, sequential effects on a broad array of behaviors.

## INTRODUCTION

Neuropeptides are thought to play a privileged role in the control of internal states. Their extended time course for signaling through G-protein coupled receptors (GPCRs) combined with their scalability of release magnitude and diffusion over long distances leaves them well poised to modulate long-lasting states[1-4]. Advances in our understanding of neuropeptidergic control over internal states and behavior have largely been driven by studies in subcortical regions[5-8]. In contrast, the contribution of neuropeptidergic signaling within cortical regions to mediate internal states remains largely unknown.

The medial prefrontal cortex (mPFC) is a social executive center in the brain, combining external information such as the age, sex, and familiarity of a conspecific with internal information about an animals current state to coordinate behavioral outputs critical for survival via "top-down" projections to downstream structures [9-13]. Output of the mPFC is controlled through a careful balance of excitation and inhibition, which is highly sensitive to changes in experience, such as stress[14-16].

One key source of stress known to impact the mPFC is social isolation (SI). Indeed, extended periods of social isolation have been shown to generate negative alterations in social behavior, including increased aggression, via its impact to reshape the mPFC[5,17-22]. Despite this knowledge, the identity of genetically defined populations of neurons in the mPFC and their functional influence over isolation-altered behaviors has been relatively unexplored. In particular, the role that neuropeptidergic populations within the mPFC play in controlling the internal state induced by prolonged SI remains unclear.

As a point of entry to determine the contribution of neuropeptidergic signaling within the mPFC to the state induced by social isolation, we focus on the neuropeptide

Tachykinin-2 (Tac2). The Tachykinin-2 system has emerged as an example of subcortically distributed, neuromodulatory control over the state induced by isolation [5]. Previous work has further implicated subcortical Tac2 in emotional and social behaviors [5,23-29]. This role for the Tachykinin-2 system seems to be evolutionarily conserved, as similar findings have been identified in *Drosophila*[29,30]

Using in-depth behavioral assessments, single nucleus RNA-sequencing, neural circuit manipulations, and CRISPR-mediated mutagenesis, we identify Tac2 neurons in the mPFC as comprising a unique, unexplored class of GABAergic interneurons, and reveal that activity of these neurons is required for isolation-induced aggression. Critical loss-of-function approaches selectively targeting the neuropeptide encoded by *Tac2*, Neurokinin B (NkB), or targeting co-release of the neurotransmitter GABA, uncover coordinated, temporally dissociable roles for these signaling molecules in the control of isolation induced-increases in both the escalation and release of aggression, respectively. Collectively, these results highlight a crucial role for neuropeptidergic signaling in the mPFC in the modulation of internal states, as well as the coordinated execution of state-induced behaviors via action of opposing signaling molecules.

## RESULTS

### Prolonged social isolation increases social investigation and induces aggression in males and females.

Chronic social isolation (> 2 weeks) has been shown to induce aggression in male mice [5,17-20,31]. To determine the impacts of prolonged social isolation (SI) across both sexes, male and female mice were isolated for two weeks and tested on the resident intruder (RI)

assay[32] (Fig 1A). Compared to group housed controls (GH), socially isolated (SI) male mice displayed an increase in the duration of time spent investigating the face of a novel conspecific (Fig 1B), or displaying a "face threat"[33], as opposed to the anogenital region or trunk of the body (Fig 1C-D). Isolated males also showed a significant upward shift in the percentage of total investigation time they allocated to both the face and anogenital regions of the intruder (Fig 1F).

In addition to changes in investigatory behaviors, SI males showed a significant increase in aggression (Fig 1E, Mann-Whitney unpaired two-tailed t-test, $p<0.05$), consistent with prior studies [5,18,29,34]. To determine whether social isolation also reshapes behavior chains, we generated behavioral transition matrices to determine the probably of transiting from one behavior to the next[35,36]. Aggressive SI males were most likely to transition from one attack bout to another (Fig G-I), suggesting that once attack is "released," attack begets attack. Interestingly, behavioral raster plots visualizing investigatory and attack bouts revealed that once attack began, anogenital and body investigation were rarely observed after the initiation of aggression (Fig 1I), suggesting that these changes in investigatory behaviors, as opposed to face threat, serve as behavioral alterations which occur leading up to aggression.

To further explore whether the onset of aggression inhibits investigation behaviors in SI mice, we examined the proportion of time aggressive SI males engaged in investigation before and after the first attack bout compared to GH males (i.e. non-fighters). We found that indeed, following the initial onset of attack, social investigation in SI males was blocked (Fig. 1 J-K, Fig S1A). Moreover, investigatory behaviors pre-attack was increased in aggressive SI mice when compared to GH counterparts (Fig 1K),

demonstrating that social isolation increases the investigatory behaviors that tile a period of aggression escalation, but that once aggression is released, escalatory behaviors are shut down.

While social isolation is well studied in males, it remains unclear how females are impacted by prolonged isolation. There is a growing body of literature showing alterations to social behavior in isolated females[16,37,38] however, female SI-aggression remains relatively unexplored. To address this, we ran female mice through the same behavioral and analysis pipeline as males (Figure 1A). Isolated females showed increased time engaged in face threat (Fig 1L), anogenital investigation (Fig 1M), and body investigation (Fig 1N). When we assessed aggression, we found that females, like males, showed isolation-induced increases in aggression towards a novel, sex-matched conspecific mouse (Fig 1O).

Interestingly, behavioral transition analyses revealed that aggressive SI females most often transition from attack to body investigation, and then back to attack (Fig 1Q). This suggests that body investigation for females may be more tightly coupled to a state of aggression. Females, like males, also displayed a significant decrease in both anogenital and body investigation after initiation of the first attack, as well as a significant increase in investigation prior to attack, when compared to GH mice (Fig 1 T-U). Like males, anogenital and body investigation, but not face threat, was rarely observed after aggression began (Fig 1S, Fig S1B).

These data highlight that while males and females display different behavioral transitions across an aggressive encounter, with unique, sex-specific precursors to aggression, isolation nevertheless generates a common state for males and females alike,

wherein both sexes demonstrate increased aggression, preceded by increased investigatory behaviors.

**mPFC Tachykinin-2 neurons represent a unique subclass of GABAergic neurons**

We previously identified a role for the neuropeptide NkB, encoded by the gene Tac2$^{+}$, in the subcortical control of the state induced by social isolation (Zelikowsky et al 2018). To determine whether this control extends to the Tac2 system in the cortex, we first determined the genetic identity of Tac2$^{+}$ cells in the mPFC, as the identity and function of this population had not been previously explored. Using single nucleus RNA sequencing as well as fluorescent in situ hybridization (RNAscope)[39], we found that Tac2 is predominately expressed in GABAergic neurons (Fig 2 A, B, Fig S2 A-C), consistent with findings in other cortical tissue [40,41]. The majority of Tac2$^{+}$cells did not overlap with a single genetic marker (Fig 2C-I) and *Tac2 was* minimally expressed in glia (Fig S2 D). The largest gene to be co-expressed with *Tac2* was VIP, which accounted for roughly half of Tac2 neurons (Fig 2C, G).

Using our RNAscope to enable spatially resolved genetic identity, we found that the majority of Tac2$^{+}$ neurons reside in layers 1-3 of cortex (Fig 2J), where they overlap with VIP by 60% (Fig 2K). These data suggest that Tac2$^{+}$ neurons are predominately localized to the early cortical layers.

To determine whether aggressive encounters were sufficient to activate mPFC Tac2$^{+}$neurons in isolated mice, we performed RNAscope for *Tac2* and cFos on GH and SI mice. We found a significant increase in cFos expressing cells for early layer Tac2$^{+}$ neurons of SI mice (Fig 2M-P). This increase was not preferentially present in Tac2$^{+}$ neurons that co-express VIP (Fig S2 F-J; S2P), suggesting that early layer Tac2$^{+}$ neurons, regardless of

VIP co-expression, are active during social encounters in SI animals compared to GH animals.

While sn-RNAseq and RNAscope provide a detailed picture of how Tac2$^+$ neurons in mPFC fit into known classes of cortical neurons, these approaches do not explain how such a small class of neurons, particularly those in the early cortical layers, could alter the mPFC to induce alterations to social behavior. Therefore, we visualized the axonal arbor of mPFC Tac2$^+$ neurons by expressing a Cre-dependent adeno-associated virus expressing membrane bound GFP and synaptophysin fused to mRuby[42] in the mPFC of Tac2-IRES-Cre mice (Fig 2Q). This anterograde tracing reveals Tac2$^+$ cell bodies primarily in layers 1-3, with axonal arbors extending into L5 of mPFC (Fig 1R), and terminals spread throughout the cortical layers, with the highest density in layer 5 (Fig 1S, T). These results illustrate the potential mPFC-wide reach of Tac2 neuron action.

**mPFC Tac2 neurons are necessary for isolation-induced aggression**

Given that Tac2$^+$ neurons in the mPFC are activated by social isolation (Fig 2), we tested whether activity of mPFC Tac2$^+$ neurons is responsible for SI-induced increases in face threat, investigation behaviors and aggression (Fig 3A). A Cre-dependent, virally encoded inhibitory DREADD virus (AAV2-hSyn-DIO-hM4D-mCherry) was injected into the mPFC of isolated, male and female Tac2-Cre mice (Fig 3B-C) to reversibly silence Tac2 neurons in the mPFC. Mice were then tested on the RI assay twice – once under the influence of the DREADDs-activating ligand, Deschloroclozapine (DCZ, 0.1mg/kg) [43], which was sufficient to silence mPFC (Fig S3F), with no off-target effects (Fig S3), and once under the influence of saline (order counter-balanced). We found that while inhibiting Tac2$^+$ mPFC neuron activity had no effect on social investigatory behaviors (Fig 3D-F),

SI-induced aggression was significantly reduced (Fig 3G). This effect was observed across both sexes (Fig S4D, H), demonstrating that in mPFC, Tac2 neuron activity is necessary for the effects of isolation to induce aggression in mice.

**Tac2 knockdown in PFC reduces isolation-induced investigation**

Tac2$^+$ neuronal activity is required for the effects of isolation to induce aggression (Fig 3), but the neurochemical mechanism underlying this effect is unknown. Our sequencing data identify Tac2$^+$ neurons as GABAergic (Fig 2), suggesting at least two potential signaling molecules which could exert control over the effects of isolation to impact behavior: release of the peptide encoded by *Tac2*, NkB, or co-release of the neurotransmitter GABA (Fig 3A). To determine the contributions of NkB signaling to isolation-induced increases in social behaviors, we used a viral mediated shRNAi to knockdown *Tac2* in the mPFC of isolated mice (Fig 4A-B) [5]. Wildtype isolated male and female mice were infused with Tac2-shRNA or a control shRNA (targeting luciferase) into the mPFC and tested on the RI assay (Fig 4A). Surprisingly, knockdown of *Tac2* in the mPFC of isolated mice resulted in a significant decrease in body investigation and a trend towards decreased anogenital investigation, while leaving face threat, the social behavior whose increase is untied to aggression (Fig 1G, Q), unaffected (Fig 4C-E; Fig S5 D, G). In contrast, *Tac2* knockdown had no impact on aggression (Fig 4F, Fig S5 A,E). These data reveal that NkB signaling contributes to the increases in investigation behaviors that lead up to aggression, but not aggression itself. Moreover, they reveal that neuropeptide signaling can exert control over behaviors that are not sensitive to a DREADD-mediated cell-silencing approach, potentially through longer term control of neuropeptide signaling across the window of isolation as well as at test.

**Disruption of GABA co-release from mPFC Tac2 neurons reduces isolation-induced aggression**

To determine whether GABA transmission from mPFC Tac2$^+$ neurons could replicate the effects of Tac2$^+$ neuron silencing (Fig 3), we used a CRISPR-based approach to generate loss-of-function (LOF) mutations in *Slc32a1*, the gene encoding the vesicular GABA transporter (vGAT), in mPFC Tac2$^+$ neurons. A viral cocktail including an AAV containing a Cre-dependent Staphylococcus aureus Cas9 (SaCas9) [44] and a guide RNA (sgRNA) directed to Slc32a1, or a control vector expressing SaCas9 and a guide RNA directed to the Rosa26 locus [45-47], was injected into the PFC of Tac2-Cre mice (Fig 5A-B). The CRIPSR virus was co-injected with a Cre-dependent cassette containing the KASH sequence fused to GFP, enabling EGFP expression in the nuclear envelope [48] and allowing visualization of the viral infusion site (Fig 5B).

Animals with the CRISPR-mediated nonsense mutation of *Slc32a1* showed no changes to social investigation behaviors (Fig 5C-E). However, the effect of isolation to induce aggression was significantly reduced in these mice (Fig 5F, Fig S6). This robust reduction in aggression, observed in both sexes, with no impact on any investigative behaviors, reveal that co-release of GABA from mPFC Tac2$^+$ neurons controls aggression, whereas NkB signaling controls investigation (Fig 5G).

**mPFC Nk3R are activated by social isolation in a cell-type specific manner**

Tac2$^+$ neurons exert influence over distinct social behaviors that span the length of an aggressive encounter following social isolation (Figs 3-5). To determine whether Tac2/NkB control is occurring locally, we assessed Nk3R cells in the mPFC.

First, to determine whether mPFC Nk3R cells, like Tac2$^{+}$ neurons, were activated by social isolation, we took an *in situ* hybridization approach to label cFos and *Tacr3*/Nk3Rs (Fig 6A). We observed no differences in cFos expression profiles for Nk3R neurons across cortical layers in SI vs. GH mice (Fig 6B two-tailed unpaired t-test, $p>0.05$). However, given that Tac2 neuronal activity varies by cortical layer in our SI mice (Fig. 2), we assessed Tacr3/Nk3R-cFos co-localization split by cortical layer. Interestingly, we saw a trend towards an increased number of active *Tacr3*/Nk3R neurons in early layers 1-3 (Fig 6C), no difference in Tacr3/Nk3R in layer 5 (Fig 6D), but a significant decrease in *Tacr3*/Nk3R activity in layer 6 (Fig 6E), compared to GH counterparts. These data suggest that isolation impacts Tacr3/Nk3R neurons differently depending on their location within the cortical layers and on which genetically defined cell type they are expressed.

To further characterize the expression of *Tacr3*/Nk3R in given cell types for GH vs. SI mice, we analyzed our sn RNAseq dataset and found that *Tacr3*/Nk3R is expressed across a diverse array of cell types of PFC (Fig 6F). When we examined the proportion *Tacr3*/Nk3R counts from excitatory and inhibitory neurons, we found a significant increase in Tacr3/Nk3R expression in inhibitory neurons of isolated animals (Fig 6G). We identified a significant increase in *Tacr3*/Nk3R expression in L2/3 excitatory neurons (Fig 6H), a trend toward decreased *Tacr3*/Nk3R expression in layer 6 excitatory Syt6$^{+}$ neurons of isolated mice (Fig 6H) and a significant decrease in *Tacr3*/Nk3R expression in L6b neurons in SI compared to GH mice (Fig 6H). We also saw a significant decrease in the proportion of L6 Car3$^{+}$ neurons expressing *Tacr3*/Nk3R in SI, compared to GH mice (Fig S6A), further supporting the notion that *Tacr3*/Nk3R expression in excitatory neurons in altered in a layer and cell type specific manner by social isolation. When we examined

*Tacr3*/Nk3R expression in GABAergic neuronal populations of mPFC, we found a significant increase in *Tacr3*/Nk3R expression in only SOM neurons (Fig 6H). As with our Tac2 analyses, we found few glial cells expressing *Tacr3*/Nk3R (Fig S7A). Lastly, we determined that Nk3R$^+$ neurons do not co-express Tac2 (Fig S7B). Collectively, these data suggest that Nk3R$^+$ cells represent a largely heterogenous population of neurons in the mPFC, whose function may largely depend on the specific sub-population of cells in which they are expressed.

Given that Nk3Rs are predominantly expressed in excitatory cells, we hypothesized that activity of these cells might similarly block isolation-induced aggression. We performed DREADD-mediated activation of these neurons in mPFC to determine whether this manipulation would alter SI-induced aggression or social behaviors (Fig 6K-O). Isolated, Nk3R-cre mice were injected with a Cre-dependent hM3D (Fig 6I-J) and tested on the RI assay. Interestingly, we found that Nk3R activation was not sufficient to generate any changes in SI-behaviors (Fig 6K-N). These results likely reflect the mixed population that Nk3R neurons represent and warrant the need for future intersectional approaches parsing out cell-type specific contributions of Nk3Rs.

## DISCUSSION

### Social Isolation induces a sex-independent, sequential pattern of increased social investigation culminating in aggression

The induction of aggression in males via social isolation is well-established in the literature[5,16,34,37,49], however this is rarely reported for females (but see [37] for exception). Here, we identified isolation-induced increases in aggression in both male and female mice.

Moreover, we found that not only does social isolation increase aggression in a sex-independent manner, but it also increased investigatory behaviors that lead up to aggression in males and females alike. Importantly, this isolation-induced increase in investigatory behavior was most pronounced during the period of social exchange preceding aggression, with investigation inhibited once animals shifted to attack behavior. The effect of isolation to promote increases in social investigation in the escalation to attack, as well as subsequently increasing attack behavior, suggests that these two sets of behaviors tile the trajectory of an aggressive encounter, consistent with the idea that once animals enter an aggressive phase, other behaviors are shut down.

Interestingly, isolation also increases face threat, which appears to be unaffected by the switch over into aggressive behavior. This suggests that face threat may be an impact of social isolation that is distinct from the effect of isolation to induce violence. Interestingly, none of our subsequent Tac2-mediated LOF perturbations had an impact on face threat, suggesting that this behavior may be controlled by a distinct signaling system operating in parallel to Tac2.

These results are consistent with a broader role for PFC in selecting behavioral responses based on internal and external information from converging inputs [9] and its general control over behavioral transitions [50,51].

**mPFC Tac2 cells represent a unique class of GABAergic interneurons**

In line with previous work in non-prefrontal cortical regions [40,52,53], we found Tac2 to be highly expressed in GABAergic neurons. We also replicated the finding that Tac2 neurons are largely located in early cortical layers, where they co-localize with VIP[52,54]. Interestingly, we found that these early layer Tac2 neurons were significantly activated in

isolated mice when compared to group housed counterparts, but that this increase was not specific to Tac2 neurons co-labelled by VIP, suggesting that isolation-sensitive Tac2 neurons represent a unique, genetically unknown class of GABAergic interneurons. While we identified Tac2 neurons to be almost exclusively GABAergic, they could nevertheless makeup a subpopulation of GABAergic cells that are not interneurons, but instead are rare, long-range GABAergic projection neurons which arise in the mPFC[55].

These findings imply that Tac2 neurons likely impact the activity of different sets of downstream neurons, including a mix of excitatory neurons and other GABAergic interneurons. It is well established that early layer (L1-3) interneurons in PFC preferentially target glutamatergic projections to the amygdala, particularly basolateral amygdala (BLA)[56,57]. Notably, there are several lines of evidence suggesting that decreased activity in PFC to BLA projections induces aggression in juvenile isolated males[16]. Thus, Tac2 neurons sit in an ideal anatomical position – and contain the appropriate genetic machinery – to enable the inhibition of long-range projection neurons (PNs) whose activity normally inhibits aggression. The idea that increased Tac2 neuron activity after social isolation could "release the brakes" of PN control over aggression is further supported by data confirming a role for activation of mPFC PNs in inhibiting aggression [16,21,58,59]. In contrast, our findings that Nk3R neurons represent a mixed population of both glutamatergic and GABAergic cell types, whose SI-induced activity depends on cortical layer, reveals that the role of Tac2/NkB signaling in controlling investigation and aggression is likely cell-type specific and cortical-layer dependent.

**Tac2/NkB exerts cortical control over isolation induced investigation**

We previously found that Tac2/NkB action within sub-cortical structures controls the state induced by isolation and its impact to promote deleterious behaviors[5]. Our targeted loss-of-function findings extend the role of Tac2/NkB beyond its function across subcortical regions, revealing a novel role for NkB signaling in the control of distinct investigation behaviors that precede aggression.

Classically, the idea that neuromodulators play a privileged role in the control of internal states has largely focused on their signaling properties in subcortical brain regions [1,8,60,61]. In contrast, the role of neuropeptides and their signaling in the cortex has been relatively understudied. Recent work has begun to reveal a role for neuromodulatory signaling in the mPFC in the control of emotional states[50], suggesting that neuromodulatory action within the cortex may be critical for the top-down control over internal states. Here, we reveal that Tac2 neuronal activity and signaling is critical for exerting control over distinct isolation-induced behaviors, investigation and aggression. To our knowledge, these data represent the first discovery of Tac2 neuron function in the cortex.

**DREADD-mediated inhibition is phenocopied by CRISPR-mediated mutagenesis of *Slc32a1***

Here we show that in the mPFC, disruption of GABA release from Tac2 neurons results in a reduction of aggression, with no impact on investigation behaviors. In contrast, shRNA-mediated knockdown of Tac2 effects investigation, but not aggression itself. These data suggest that NkB controls social investigatory behaviors that lead up to aggression, but not aggression itself, while co-release of GABA from the same Tac2 neurons controls aggression itself. Interestingly, DREADD-mediated inhibition of Tac2 neurons reduces

aggression, but has no effect on investigation, thereby phenocopying the effects of disrupting GABA signaling from Tac2 neurons, but not the effects of Tac2 knockdown within the same cells. We reason that this may be due to the nature of our chemogenetic LOF approach, as there is evidence that hM4Di DREADDs not only hyperpolarize neurons via G-protein-gated inwardly rectifying potassium (GIRK) channels but are also able to inhibit neurotransmitter release through the βγ subunit's interaction with the SNARE protein, SNAP-25 [62,63], potentially explaining the effects of this approach to disrupt GABAergic signaling but not NP signaling. While there is evidence that SNAP-25 is part of neuropeptidergic dense core vesicle (DCV) fusion and release[64,65], it remains understudied, making it difficult to assess whether hM4Di-mediated neuronal inhibition would impact neuropeptide release. Additional LOF approaches are warranted to further explore whether mPFC Tac2 neuron activity is required for isolation-induced increases in investigatory behaviors.

**Implications for the treatment of pathological aggression**

Aggression is a social behavior, critical for survival. However, when elicited in excess or as a result of stress, aggression can become pathological. As with other forms of pathological behavior the mPFC is thought to offer promise as a region capable of exerting top-down control over aggression[66,67]. Here, we identify the neuropeptide, Tac2, as a critical player in the circuitry of isolation induced aggression – not just subcortically, but in the cortex as well. We find that Tac2 cells in the mPFC enable a delicate balance between the behaviors displayed during an aggressive encounter in response to social isolation. These findings suggest a target region, and target molecule, for the control of isolation-

induced aggression, and reveal novel motifs for the coordinated control of sequential behaviors.

## METHODS

### Animals

Wild-type (WT) C57BL/6N male and female mice and BALB/C intruders (male and female) were obtained from Charles River (7-10 weeks of age). For Cre-dependent viral manipulation experiments, we used the Tac2-IRES-Cre strain [68] and the Tacr3$^{iCre:GFP}$ (Jackson labs) which were backcrossed to C57BL/6N at the University of Utah animal facility. Mice were housed and maintained on a reverse 12-hr light-dark cycle with food and *water ad libitium*. All behavior testing was performed during the dark cycle. Experimental manipulations and animal care were performed following the National Institutes of Health Guide for Care and Use of Laboratory Animals and approved by the University of Utah Institutional Animal Care and Use Committee.

### Resident Intruder assay

8-10-week-old C57Bl6/N mice (Charles River, strain code: 027) were either single housed or remained group housed in cages of four for two weeks. For the Resident Intruder (RI) assay, mice were transferred to the behavioral testing room and allowed to acclimate in the dark for approximately 30 minutes before the start of testing. Isolated mice remained in their home cage for the duration of testing. To begin animals were placed under an infrared Basler camera for and video recorded for three minutes as a baseline, then an age- and sex- matched Balb/c (Charles River, strain code: 028) intruder was then placed in the cage for 10 minutes as the test phase. For group housed animals, untested cage mates were

removed from the home cage and placed in a clean holding cage, then once a given animal had been tested it was moved to a clean holding cage with its tested cage mates. Following the completion of testing for all mice in each cage, the mice were returned to their home cage. The apparatus was cleaned with 70% ethanol between all tests to reduce olfactory cues.

Behavior scoring

All behavior (attack, mounting, face investigation, body investigation, anogenital investigation) were scoring by a trained, blinded observer using Noldus Observer, data was then exported to Excel (Microsoft).

Transition matrices

The transition matrices were generated by calculating the probably of a mouse transition from one behavior to the next within a one second window of time, see [36].

**RNAscope (fluorescent in situ hybridization)**

For cFos RNAscope™ experiments mice were anesthetized using isoflurane (4-5%), animals were rapidly decapitated, and brains extracted 30 minutes from the start of the test phase of the RI assay. Brains were placed into cold 2-methylbutane (Sigma-Aldrich, M32631-4L) for approximately ten seconds or until frozen, then wrapped in foil and stored at -80°C for cryo-Sectioning. For RNAscope protocol see below section.

Brains were rapidly extracted and flash frozen in 2-methylbutane (Sigma-Aldrich, catalog #: M32631-4L) and stored at -80C for up to 4 months. Sections were taken at 20µm thick and mounted directly onto slides (SuperFrost PLUS Adhesion slide, Electron Microscopy Sciences, catalog #: 71869-11) in the cryostat. Roughly 4-5 sections from two animals, one per housing condition were placed on each slide. Slides were stored in airtight

containers at -80°C for up to four months before the RNAscope™ assay was performed. The RNAscope™ assay was performed according to the manufacturer's instructions (Advanced Cell Diagnostics, see Wang et al 2012). The following probes (ACDBio) were used: Tac2, PVALB, SOM, cFos, Tacr3, VIP, CRH, GAD1, GAD2, SLCA717, SLC32A1 The slides were then imaged on a Keyence BX-X800 within a week of the assay.

**Single nucleus RNA sequencing**

The mPFC (prelimbic and infralimbic) was dissected form three group housed and three isolated C57Bl/6N males (strain code: 027, isolated for three weeks) in ice cold RNase free 1X PBS containing 15um actinomyocin-D [69] (Sigma-Aldrich, catalog #A1410-10MG). Nuclei were isolated using manual homogenization and the Nuclei PURE Prep kit (Millipore Sigma, catalog # NUC201-1KT) with 15 μM actinomycin-D added to the lysis buffer. Nuclei were resuspended in a resuspension buffer containing 0.5% Ultrapure BSA (Fisher Scientific #AM2616) to prevent clumping of nuclei and 0.2 U/μl RNase inhibitor (New England Biolabs #M0314S) to prevent RNA degradation [70]. Single-nuclei barcoded cDNA libraries were generated by the University of Utah High Throughput Sequencing using the 10x Genomics user guide "Chromium Next GEM Single Cell 3' Reagent Kits v3.1". Libraries were sequenced on the Illumina NovaSeq 6000. Fastq files were aligned to the GRCm39 reference genome using 10X Cell Ranger (v4.0.8). Filtered gene expression matrices were then imported into R (v4.3.0) and nuclei with fewer than 800 features, greater than 6000 features, or greater than 5% mitochondrial reads were removed to eliminate low quality nuclei and multiplets. Seurat (v4.2.1)[71] was used to calculate nearest neighbors at 0.8 resolution from the first 30 principal components and cluster nuclei

using UMAP dimensionality reduction. Then clusters were assigned to known cell types based on expression of known cell type specific marker genes [53,72].

**Surgical procedures**

Mice were anesthetized in an induction chamber using 4-5% isoflurane and anesthesia was maintained at 1-2% for the duration of the procedure while mice were mounted on the nose cone of the stereotaxic surgery rig (Kopf Instruments, California, USA). Once mounted in the nose cone, ophthalmic ointment (Soothe lubricant eye ointment, Bausch and Lomb) was applied to prevent eyes from during the procedure. Topical hair removal cream (Nair) was applied to the scalp to remove hair, following removal of cream and wiping with distilled water, the surgical area was cleaned 3x with povidone-iodine solution (Dynarex, catalog 1415) and isopropyl alcohol (Solimo). A subcutaneous injection of sustained release buprenorphine at a dose of 3.25 mg/kg animal weight (Ethiqa XR 1.3mg/ l mL, Fidelis Animal Health) was given before incisions to provide analgesia. A small incision was made along the scalp to expose the skull, and the skull was leveled between bregma and lambda as well as in the medial/lateral direction. Holes were then drilled at the coordinates for the viral infusion cites.

All infusion coordinates into the medial prefrontal cortex (infralimbic) were made in relation to brain in mm. For all experiments (DREADDs, Tac2 shRNA, visualization of Tac2 neuron morphology, CRISPR mutagenesis) bilateral infusions were performed at AP: +2.14, ML: +/- 0.25, DV: -2.79. Virus was backfilled into pulled fine glass capillaries (~ 50 μm diameter tip; World Precision Instruments, item no. 504949) filled with mineral oil (sigma Aldrich, M5904, CAS 8042-47-5) and 140nL virus (each side) was infused at a rate of 80nL/min using a nanoliter injector (Nanoliter 2000, World Precision Instruments)

controlled by an ultra-micro-syringe pump (Micro4, World Precision Instruments). Capillaries remained in place for 5 minutes following viral infusion to allow for full diffusion of virus and to reduce backflow up the infusion tract. The scalp was drawn together and sealed with GLUture (World Precision Instruments, catalog 503763). All infusion sites were verified using epifluorescent microscopy.

**Characterization of Dendritic Arbor of mPFC Tac2 neurons**

Male and female Tac2-IRES-Cre mice 8-10 weeks were single housed and had surgeries performed to infuse a Cre-dependent adeno-associated virus (AAV) expressing membrane-GFP and synaptophysin fused to mRuby (AAV2-hSynb-FLEx-mGFP-2A-Synaptophysin-mRuby) infused into the mPFC (Addgene #: 71760-AAV2, titer: 2.7 x $10^{12}$ GC/mL, lot: v138755). Virus was allowed to express for approximately four weeks, then animals anesthetized with isoflurane (4-5%) and rapidly decapitated. Brains were post fixed in 4% paraformaldehyde (CAS 30525-89-4, Sigma Aldrich, catalog #: 158127-500G) overnight at 4°C, then transferred to 15% sucrose overnight at 4°C, followed by 30% sucrose overnight at 4°C. After the final sucrose transfer brains were embedded in OCT (Tissue-Tek O.C.T Compound, Sakura Finetek USA Inc, catalog #: 4583) and stored at -80° until cryo-sectioning. Viral placement and expression were verified for all animals using epifluorescent microscopy.

**DREADD mediated inhibition and activation**

Male and female Tac2-IRES-Cre and Tacr3$^{iCreGFP:}$ mice were single housed starting at 8-10 weeks of age for three weeks to induce social isolation, then the Resident Intruder assay was used to screen for attack. The pre-screening test was a shortened RI paradigm

with a two-minute baseline and 8-minute test phase, mice showing any aggressive behavior (attack, mounting) were considered "aggressive." Animals that showed at least one attack bout were then used for neural manipulation experiments. To manipulate the activity of Tac2 and Nk3R neurons in the mPFC of mice, Cre-dependent DREADDs constructs were infused into the mPFC of Tac2-IRES-Cre (Jackson laboratories, strain#: 021878) and Tacr3$^{iCre:GFP}$ (gift from Palmiter lab, University of Washington, Jax strain #: 035576) via stereotaxic surgery. Mice were anesthetized with 4% isoflurane (MWI Animal Health, VetOne, MWI #: 502017) and mounted on a stereotaxic frame with a nose cone for anesthesia. In Tac2-IRES-Cre mice, 140nL of a Cre-dependent inhibitory DREADDs virus (AAV2-hSyn-DIO-hM4Di-mCherry, Addgene # 44362, titer 3.3x10$^{13}$ GC/mL, lot v138755 ) was infused bilaterally into the of aggressive Tac2-IRES-cre mice. An identical protocol was used for Tacr3$^{iCre:GFP}$ mice, except a virus encoding the excitatory DREADD (AAV2-hSyn-DIO-hM3D-mCherry, (Addgene #44361-AAV2; titer 1.08 x 10$^{13}$GC/mL, lot: v129215) was infused. Following surgeries mice remained single housed for three to four weeks before Resident intruder.

For behavioral testing, Tac2-IRES-Cre and Tacr3$^{iCre:GFP}$ mice received 0.1 mg/kg body weight Deschloroclozapine (DCZ, CAS: 9177-07-7, MedChemExpress, catalog #: HY-42110) or vehicle (DMSO/saline) via intraperitoneal injection 10 minutes before the start of the baseline phase of the RI assay (see above for detailed information). Mice were randomly assigned to receive a given drug on a given day so for each round of behavior testing there were approximately even numbers of mice receiving DCZ on the first day and vehicle on the first day. After the first test mice were administered the other solution, i.e. if the animal received DCZ on the first test day, they then received the vehicle solution on

the second test day 48hrs after the first test day. Video was recorded during baseline and test phases in infrared light using a high-speed Basler camera. Following behavior, brains were taken and post-fixed in 4% Paraformaldehyde (CAS 30525-89-4, Sigma Aldrich, catalog #: 158127-500G) overnight at 4°C, then transferred to 15% sucrose overnight at 4C, followed by 30% sucrose overnight at 4°C. After the final sucrose transfer brains were embedded in OCT (Tissue-Tek O.C.T Compound, Sakura Finetek USA Inc, catalog #: 4583) and stored at -80° until cryo-sectioning. Viral placement and expression were verified for all animals using epifluorescent microscopy.

To determine whether DCZ had off-target effects on mouse behavior in the resident intruder assay, male and female WT littermates of animals from the Tac2-IRES-Cre and Tacr3$^{iCre:GFP}$ colonies were injected with two of four doses of DCZ (0.1mg/kg, 0.25mg/kg, 0.5 mg/kg or 1.0 mg/kg body weight) to account for variability in animal behavior. The days on which animals received vehicle or DCZ was counterbalanced. The behavioral testing on RI occurred just as in the DREADDs experiments, with the exception that mice were tested on the second dose of DCZ approximately one week after the first two test days.

Statistical analysis on the duration of behaviors on vehicle and DCZ was performed using GraphPad PRSIM. Only animals that engaged in aggression (mounting, attack) on at least one of the test days were included in the analyses. Normality tests and QQ plots were performed, and a Wilcoxon test was performed if data was not normally distributed, if data was normally distributed then a paired t-test was performed.

**Immunohistochemistry**

For cFos immunohistochemistry experiments, mice underwent transcardial perfusions with 0.9% saline (MWI Animal Health, catalog # 033500) followed by 4% paraformaldehyde (PFA; Paraformaldehyde powder, CAS 30525-89-4, Sigma Aldrich, catalog #: 158127-500G) 90 minutes after the middle of the test phase of the Resident Intruder assay and post-fixed in 4% (PFA) overnight at 4°C. Brains were then transferred to 15% sucrose solution (Sigma-Aldrich, S0389-5KG, CAS 57-50-1) at 4°C overnight. Then brains were then transferred to 30% sucrose solution overnight at 4°. Brains were then sectioned at 40um into 1X PBS (Gibco, ref 10010-023) and stored at 4C for up to a week before immunohistochemistry was performed. Sections were incubated in 10% Normal Donkey Serum (Sigma-Aldrich, catalog #: D9663-10mL) + 0.3% Triton X-100 (Sigma, X-100) in 1X PBS (Gibco, ref 10010-023) for one hour at room temperature. Then sections were incubated in the primary antibody (rabbit anti-cFos, Abcam 190289) at 4°C for 72 hrs. Following this incubation, sections were rinsed in 1X PBS (Gibco, ref 10010-023) three times then incubated in secondary antibody (Donkey anti-rabbit Alexa Fluor-488, 1:250 dilution in blocking buffer, catalog A-21206, ThermoFisher) for 12 hours. After this period, sections were rinsed three times in 1X PBS (Gibco, ref 10010-023), then mounted onto slides (SuperFrost PLUS Adhesion slide, Electron Microscopy Sciences, catalog #: 71869-11) and counterstained with DAPI mounting media (DAPI Fluoromount-G Mounting Medium, Liquid, Southern Biotech, catalog # 0100-20). Slides were imaged with epifluorescent microscope (Keyence BX-Z800) by a blinded experimenter within seven days of mounting. The number of $cFos^{+}$ cells and total number of cells (DAPI) were quantified on sections with viral expression in mPFC (FIJI). GraphPad PRISM was used

to perform the nested t-tests for the number cFos$^{+}$ cells out the total number of cells on tissue from each drug condition.

**Tac2 shRNA experiments**

Male and female 8-week-old C57Bl6/N mice (Charles River, strain code: 027) were single housed for two-three weeks, then pre-screened for aggression. Aggressive mice were randomly assigned two approximately equal sized groups and infused with either the Tac2 shRNA virus or a luciferase control virus (plasmids courtesy of Tomomi Karigo and David Anderson; see Zelikowsky et al 2018) into the mPFC. After three weeks of expression and recovery, animals were tested on the Resident Intruder assay. Statistical analysis for the duration for behaviors between shLuciferase vs shTac2 animals was performed using GraphPad PRISM. Normality tests were performed for the data in each behavior category and unpaired t-tests were performed (normally distributed: unpaired t-test, not normally distributed: Mann-Whitey test).

Following the completion of behavioral testing, brains were flash frozen within three days and sectioned in preparation for RNAscope™. For the RNAscope™, each slide contained two mice, one from each viral condition, and the Tac2 probe was used to examine for Tac2 knockdown. Slides were imaged using the Keyence BX-Z800. Experimenters were blinded to both the sex and viral condition of animals during RNAscope™, imaging, behavior scoring and cell counting. Knockdown of Tac2 was verified by taking automated counts of DAPI and manual counts of Tac2 (quantified by fluorescence in Tac2 channel that co-localized with DAPI signal) in FIJI. GraphPad PRIM was used for nested t-test of cell count data. Viral placement and expression were verified for all animals using epifluorescent microscopy.

**CRISPR mutagenesis experiments**

Male and female 8 – 10-week-old Tac2-IRES-Cre mice received bilateral infusions of a 1 EGFP-KASH: 9 parts saCas9 mixture of either AAV1-FLEX-saCas9-U6-sgSlc32a1 and AAV1-EGFP-KASH or AAV1-FLEX-saCas9-U6-Rosa26 and AAV1-EGFP-KASH (Gift from Zweifel lab). Following surgery mice were single housed for four weeks to allow for viral expression. After this period, mice were tested on the Resident Intruder assay as described above and blinded experimenters scored behavior (Noldus Observer) to quantify to duration of aggression, face investigation, anogenital investigation and body investigation. Data was then analyzed in GraphPad PRISM, normality tests were performed and for all data that was not normally distributed, Mann-Whitney tests were performed and unpaired t-tests were performed on normally distributed data.

Brains were extracted within a week of behavioral testing, post-fixed in 4% paraformaldehyde at 4°C overnight, then 15% sucrose and 30% overnight before embedding in OCT (Tissue-Tek O.C.T Compound, Sakura Finetek USA Inc, catalog #: 4583) and storage at -80°C. Cryo-sectioning was performed and the presence and location of virus in the brain was recorded using epifluorescent microscopy by a blinded experimenter.

**ACKNOWLEDGMENTS**

We thank Bai Luo, Director of the Drug Discovery Core Facility at the University of Utah for their assistance in packaging shRNA plasmids into adeno-associated viral envelopes; the University of Utah Machine Shop for building the Resident Intruder assay boxes; Dr. Larry Zweifel for the viruses for the CRISPR vGAT experiments; Dr. Kristen Keefe for her guidance on RNAscope experiments and analysis; Becky Dennis for assistance with cryosectioning brains. This work was supported by the National Institutes of Mental Health (RG 1F31MH131359-01,02,03; MZ R01 MH132822), a Klingenstein-Simmons Early Investigator Award (MZ), a Whitehall Fellowship (MZ), a Sloan Fellowship (MZ), a McKnight Scholars Award (MZ) and the University of Utah.

**REFERENCES**


1. Flavell, S.W., Gogolla, N., Lovett-Barron, M., and Zelikowsky, M. (2022). The emergence and influence of internal states. Neuron *110*, 2545-2570. 10.1016/j.neuron.2022.04.030.
2. van den Pol, A.N. (2012). Neuropeptide transmission in brain circuits. Neuron *76*, 98-115. 10.1016/j.neuron.2012.09.014.
3. Zelikowsky, M., Ding, K., and Anderson, D.J. (2018). Neuropeptidergic Control of an Internal Brain State Produced by Prolonged Social Isolation Stress. Cold Spring Harb Symp Quant Biol *83*, 97-103. 10.1101/sqb.2018.83.038109.
4. Flavell, S.W., Pokala, N., Macosko, E.Z., Albrecht, D.R., Larsch, J., and Bargmann, C.I. (2013). Serotonin and the neuropeptide PDF initiate and extend opposing behavioral states in C. elegans. Cell *154*, 1023-1035. 10.1016/j.cell.2013.08.001.
5. Zelikowsky, M., Hui, M., Karigo, T., Choe, A., Yang, B., Blanco, M.R., Beadle, K., Gradinaru, V., Deverman, B.E., and Anderson, D.J. (2018). The Neuropeptide Tac2 Controls a Distributed Brain State Induced by Chronic Social Isolation Stress. Cell *173*, 1265-1279.e1219. 10.1016/j.cell.2018.03.037.
6. Asede, D., Doddapaneni, D., and Bolton, M.M. (2022). Amygdala Intercalated Cells: Gate Keepers and Conveyors of Internal State to the Circuits of Emotion. J Neurosci *42*, 9098-9109. 10.1523/jneurosci.1176-22.2022.
7. Allen, W.E., Chen, M.Z., Pichamoorthy, N., Tien, R.H., Pachitariu, M., Luo, L., and Deisseroth, K. (2019). Thirst regulates motivated behavior through modulation of brainwide neural population dynamics. Science *364*, 253. 10.1126/science.aav3932.
8. Soden, M.E., Yee, J.X., and Zweifel, L.S. (2023). Circuit coordination of opposing neuropeptide and neurotransmitter signals. Nature *619*, 332-337. 10.1038/s41586-023-06246-7.
9. Yizhar, O., and Levy, D.R. (2021). The social dilemma: prefrontal control of mammalian sociability. Curr Opin Neurobiol *68*, 67-75. 10.1016/j.conb.2021.01.007.
10. Chen, P., and Hong, W. (2018). Neural Circuit Mechanisms of Social Behavior. Neuron *98*, 16-30. 10.1016/j.neuron.2018.02.026.
11. Arnsten, A.F. (2009). Stress signalling pathways that impair prefrontal cortex structure and function. Nat Rev Neurosci *10*, 410-422. 10.1038/nrn2648.
12. Padilla-Coreano, N., Batra, K., Patarino, M., Chen, Z., Rock, R.R., Zhang, R., Hausmann, S.B., Weddington, J.C., Patel, R., Zhang, Y.E., et al. (2022). Cortical ensembles orchestrate social competition through hypothalamic outputs. Nature *603*, 667-671. 10.1038/s41586-022-04507-5.
13. Cum, M., Santiago Pérez, J.A., Wangia, E., Lopez, N., Wright, E.S., Iwata, R.L., Li, A., Chambers, A.R., and Padilla-Coreano, N. (2024). A systematic review and meta-analysis of how social memory is studied. Sci Rep *14*, 2221. 10.1038/s41598-024-52277-z.
14. Yizhar, O., Fenno, L.E., Prigge, M., Schneider, F., Davidson, T.J., O'Shea, D.J., Sohal, V.S., Goshen, I., Finkelstein, J., Paz, J.T., et al. (2011). Neocortical

excitation/inhibition balance in information processing and social dysfunction. Nature *477*, 171-178. 10.1038/nature10360.

15. Liu, L., Xu, H., Wang, J., Li, J., Tian, Y., Zheng, J., He, M., Xu, T.L., Wu, Z.Y., Li, X.M., et al. (2020). Cell type-differential modulation of prefrontal cortical GABAergic interneurons on low gamma rhythm and social interaction. Sci Adv *6*, eaay4073. 10.1126/sciadv.aay4073.
16. Tan, T., Wang, W., Liu, T., Zhong, P., Conrow-Graham, M., Tian, X., and Yan, Z. (2021). Neural circuits and activity dynamics underlying sex-specific effects of chronic social isolation stress. Cell Rep *34*, 108874. 10.1016/j.celrep.2021.108874.
17. Biro, L., Miskolczi, C., Szebik, H., Bruzsik, B., Varga, Z.K., Szente, L., Toth, M., Halasz, J., and Mikics, E. (2023). Post-weaning social isolation in male mice leads to abnormal aggression and disrupted network organization in the prefrontal cortex: Contribution of parvalbumin interneurons with or without perineuronal nets. Neurobiol Stress *25*, 100546. 10.1016/j.ynstr.2023.100546.
18. Li, X., Sun, H., Zhu, Y., Wang, F., Wang, X., Han, L., Cui, D., Luo, D., Zhai, Y., Zhuo, L., et al. (2022). Dysregulation of prefrontal parvalbumin interneurons leads to adult aggression induced by social isolation stress during adolescence. Front Mol Neurosci *15*, 1010152. 10.3389/fnmol.2022.1010152.
19. Chaibi, I., Bennis, M., and Ba-M'Hamed, S. (2021). GABA-A receptor signaling in the anterior cingulate cortex modulates aggression and anxiety-related behaviors in socially isolated mice. Brain Res *1762*, 147440. 10.1016/j.brainres.2021.147440.
20. Wang, Z.J., Shwani, T., Liu, J., Zhong, P., Yang, F., Schatz, K., Zhang, F., Pralle, A., and Yan, Z. (2022). Molecular and cellular mechanisms for differential effects of chronic social isolation stress in males and females. Mol Psychiatry *27*, 3056-3068. 10.1038/s41380-022-01574-y.
21. Heukelum, S.V., Geers, F.E., Tulva, K., van Dulm, S., Beckmann, C.F., Buitelaar, J.K., Glennon, J.C., Vogt, B.A., Havenith, M.N., and França, A.S.C. (2021). Structural Degradation in Midcingulate Cortex Is Associated with Pathological Aggression in Mice. Brain Sci *11*. 10.3390/brainsci11070868.
22. Bicks, L.K., Yamamuro, K., Flanigan, M.E., Kim, J.M., Kato, D., Lucas, E.K., Koike, H., Peng, M.S., Brady, D.M., Chandrasekaran, S., et al. (2020). Prefrontal parvalbumin interneurons require juvenile social experience to establish adult social behavior. Nat Commun *11*, 1003. 10.1038/s41467-020-14740-z.
23. Florido, A., Velasco, E.R., Soto-Faguás, C.M., Gomez-Gomez, A., Perez-Caballero, L., Molina, P., Nadal, R., Pozo, O.J., Saura, C.A., and Andero, R. (2021). Sex differences in fear memory consolidation via Tac2 signaling in mice. Nat Commun *12*, 2496. 10.1038/s41467-021-22911-9.
24. Zhao, Z.D., Han, X., Chen, R., Liu, Y., Bhattacherjee, A., Chen, W., and Zhang, Y. (2022). A molecularly defined D1 medium spiny neuron subtype negatively regulates cocaine addiction. Sci Adv *8*, eabn3552. 10.1126/sciadv.abn3552.
25. Hook, M., Xu, F., Terenina, E., Zhao, W., Starlard-Davenport, A., Mormede, P., Jones, B.C., Mulligan, M.K., and Lu, L. (2019). Exploring the involvement of Tac2 in the mouse hippocampal stress response through gene networking. Gene *696*, 176-185. 10.1016/j.gene.2019.02.013.

26. Andero, R., Dias, B.G., and Ressler, K.J. (2014). A role for Tac2, NkB, and Nk3 receptor in normal and dysregulated fear memory consolidation. Neuron *83*, 444-454. 10.1016/j.neuron.2014.05.028.
27. Andero, R., Daniel, S., Guo, J.D., Bruner, R.C., Seth, S., Marvar, P.J., Rainnie, D., and Ressler, K.J. (2016). Amygdala-Dependent Molecular Mechanisms of the Tac2 Pathway in Fear Learning. Neuropsychopharmacology : official publication of the American College of Neuropsychopharmacology *41*, 2714-2722. 10.1038/npp.2016.77.
28. Boyle, C.A., Hu, B., Quaintance, K.L., Mastrud, M.R., and Lei, S. (2022). Ionic signalling mechanisms involved in neurokinin-3 receptor-mediated augmentation of fear-potentiated startle response in the basolateral amygdala. J Physiol *600*, 4325-4345. 10.1113/jp283433.
29. Asahina, K., Watanabe, K., Duistermars, B.J., Hoopfer, E., González, C.R., Eyjólfsdóttir, E.A., Perona, P., and Anderson, D.J. (2014). Tachykinin-expressing neurons control male-specific aggressive arousal in Drosophila. Cell *156*, 221-235. 10.1016/j.cell.2013.11.045.
30. Asahina, K., and Zelikowsky, M. (2025). Comparative perspectives on neuropeptide function and social isolation. Biological Psychiatry. https://doi.org/10.1016/j.biopsych.2025.01.019.
31. Myers, T., Birmingham, E.A., Rhoads, B.T., McGrath, A.G., Miles, N.A., Schuldt, C.B., and Briand, L.A. (2024). Post-weaning social isolation alters sociability in a sex-specific manner. Front Behav Neurosci *18*, 1444596. 10.3389/fnbeh.2024.1444596.
32. Thurmond, J.B. (1975). Technique for producing and measuring territorial aggression using laboratory mice. Physiol Behav *14*, 879-881. 10.1016/0031-9384(75)90086-4.
33. Blanchard, R.J., Wall, P.M., and Blanchard, D.C. (2003). Problems in the study of rodent aggression. Hormones and Behavior *44*, 161-170. https://doi.org/10.1016/S0018-506X(03)00127-2.
34. Oliveira, V.E.M., Evrard, F., Faure, M.C., and Bakker, J. (2024). Social isolation and aggression training lead to escalated aggression and hypothalamus-pituitary-gonad axis hyperfunction in mice. Neuropsychopharmacology *49*, 1266-1275. 10.1038/s41386-024-01808-3.
35. Chen, C., Altafi, M., Corbu, M.-A., Trenk, A., van den Munkhof, H., Weineck, K., Bender, F., Carus-Cadavieco, M., Bakhareva, A., Korotkova, T., and Ponomarenko, A. (2024). The dynamic state of a prefrontal–hypothalamic–midbrain circuit commands behavioral transitions. Nature Neuroscience *27*, 952-963. 10.1038/s41593-024-01598-3.
36. Ahmadlou, M., Houba, J.H.W., van Vierbergen, J.F.M., Giannouli, M., Gimenez, G.A., van Weeghel, C., Darbanfouladi, M., Shirazi, M.Y., Dziubek, J., Kacem, M., et al. (2021). A cell type-specific cortico-subcortical brain circuit for investigatory and novelty-seeking behavior. Science *372*. 10.1126/science.abe9681.
37. Pinna, G., Dong, E., Matsumoto, K., Costa, E., and Guidotti, A. (2003). In socially isolated mice, the reversal of brain allopregnanolone down-regulation

mediates the anti-aggressive action of fluoxetine. Proceedings of the National Academy of Sciences *100*, 2035-2040.

38. Morè, L. (2008). Intra-female aggression in the mouse (Mus musculus domesticus) is linked to the estrous cycle regularity but not to ovulation. Aggress Behav *34*, 46-50. 10.1002/ab.20217.
39. Wang, F., Flanagan, J., Su, N., Wang, L.C., Bui, S., Nielson, A., Wu, X., Vo, H.T., Ma, X.J., and Luo, Y. (2012). RNAscope: a novel in situ RNA analysis platform for formalin-fixed, paraffin-embedded tissues. J Mol Diagn *14*, 22-29. 10.1016/j.jmoldx.2011.08.002.
40. Gallopin, T., Geoffroy, H., Rossier, J., and Lambolez, B. (2006). Cortical sources of CRF, NKB, and CCK and their effects on pyramidal cells in the neocortex. Cereb Cortex *16*, 1440-1452. 10.1093/cercor/bhj081.
41. Yao, Z., van Velthoven, C.T.J., Nguyen, T.N., Goldy, J., Sedeno-Cortes, A.E., Baftizadeh, F., Bertagnolli, D., Casper, T., Chiang, M., Crichton, K., et al. (2021). A taxonomy of transcriptomic cell types across the isocortex and hippocampal formation. Cell *184*, 3222-3241.e3226. https://doi.org/10.1016/j.cell.2021.04.021.
42. Beier, K.T., Steinberg, E.E., DeLoach, K.E., Xie, S., Miyamichi, K., Schwarz, L., Gao, X.J., Kremer, E.J., Malenka, R.C., and Luo, L. (2015). Circuit Architecture of VTA Dopamine Neurons Revealed by Systematic Input-Output Mapping. Cell *162*, 622-634. 10.1016/j.cell.2015.07.015.
43. Nagai, Y., Miyakawa, N., Takuwa, H., Hori, Y., Oyama, K., Ji, B., Takahashi, M., Huang, X.-P., Slocum, S.T., DiBerto, J.F., et al. (2020). Deschloroclozapine, a potent and selective chemogenetic actuator enables rapid neuronal and behavioral modulations in mice and monkeys. Nature Neuroscience *23*, 1157-1167. 10.1038/s41593-020-0661-3.
44. Hunker, A.C., Soden, M.E., Krayushkina, D., Heymann, G., Awatramani, R., and Zweifel, L.S. (2020). Conditional Single Vector CRISPR/SaCas9 Viruses for Efficient Mutagenesis in the Adult Mouse Nervous System. Cell Rep *30*, 4303-4316.e4306. 10.1016/j.celrep.2020.02.092.
45. Friedrich, G., and Soriano, P. (1991). Promoter traps in embryonic stem cells: a genetic screen to identify and mutate developmental genes in mice. Genes Dev *5*, 1513-1523. 10.1101/gad.5.9.1513.
46. Josh Huang, Z., and Zeng, H. (2013). Genetic approaches to neural circuits in the mouse. Annual review of neuroscience *36*, 183-215.
47. Zambrowicz, B.P., Imamoto, A., Fiering, S., Herzenberg, L.A., Kerr, W.G., and Soriano, P. (1997). Disruption of overlapping transcripts in the ROSA βgeo 26 gene trap strain leads to widespread expression of β-galactosidase in mouse embryos and hematopoietic cells. Proceedings of the National Academy of Sciences *94*, 3789-3794.
48. Swiech, L., Heidenreich, M., Banerjee, A., Habib, N., Li, Y., Trombetta, J., Sur, M., and Zhang, F. (2015). In vivo interrogation of gene function in the mammalian brain using CRISPR-Cas9. Nature biotechnology *33*, 102-106.
49. Ross, A.P., McCann, K.E., Larkin, T.E., Song, Z., Grieb, Z.A., Huhman, K.L., and Albers, H.E. (2019). Sex-dependent effects of social isolation on the regulation of arginine-vasopressin (AVP) V1a, oxytocin (OT) and serotonin

(5HT) 1a receptor binding and aggression. Horm Behav *116*, 104578. 10.1016/j.yhbeh.2019.104578.

50. Wang, H., Flores, R.J., Yarur, H.E., Limoges, A., Bravo-Rivera, H., Casello, S.M., Loomba, N., Enriquez-Traba, J., Arenivar, M., Wang, Q., et al. (2024). Prefrontal cortical dynorphin peptidergic transmission constrains threat-driven behavioral and network states. Neuron *112*, 2062-2078.e2067. 10.1016/j.neuron.2024.03.015.
51. Chen, C., Altafi, M., Corbu, M.A., Trenk, A., van den Munkhof, H., Weineck, K., Bender, F., Carus-Cadavieco, M., Bakhareva, A., Korotkova, T., and Ponomarenko, A. (2024). The dynamic state of a prefrontal-hypothalamic-midbrain circuit commands behavioral transitions. Nat Neurosci *27*, 952-963. 10.1038/s41593-024-01598-3.
52. Kaneko, T., Murashima, M., Lee, T., and Mizuno, N. (1998). Characterization of neocortical non-pyramidal neurons expressing preprotachykinins A and B: a double immunofluorescence study in the rat. Neuroscience *86*, 765-781. 10.1016/s0306-4522(98)00036-0.
53. Yao, Z., van Velthoven, C.T.J., Nguyen, T.N., Goldy, J., Sedeno-Cortes, A.E., Baftizadeh, F., Bertagnolli, D., Casper, T., Chiang, M., Crichton, K., et al. (2021). A taxonomy of transcriptomic cell types across the isocortex and hippocampal formation. Cell *184*, 3222-3241.e3226. 10.1016/j.cell.2021.04.021.
54. Wu, J., Zhao, Z., Shi, Y., and He, M. (2022). Cortical VIP(+) Interneurons in the Upper and Deeper Layers Are Transcriptionally Distinct. J Mol Neurosci *72*, 1779-1795. 10.1007/s12031-022-02040-8.
55. Bai, F., Huang, L., Deng, J., Long, Z., Hao, X., Chen, P., Wu, G., Wen, H., Deng, Q., Bao, X., et al. (2023). Prelimbic area to lateral hypothalamus circuit drives social aggression. iScience *26*, 107718. 10.1016/j.isci.2023.107718.
56. Anastasiades, P.G., and Carter, A.G. (2021). Circuit organization of the rodent medial prefrontal cortex. Trends Neurosci *44*, 550-563. 10.1016/j.tins.2021.03.006.
57. McGarry, L.M., and Carter, A.G. (2016). Inhibitory Gating of Basolateral Amygdala Inputs to the Prefrontal Cortex. J Neurosci *36*, 9391-9406. 10.1523/jneurosci.0874-16.2016.
58. Takahashi, A., Nagayasu, K., Nishitani, N., Kaneko, S., and Koide, T. (2014). Control of intermale aggression by medial prefrontal cortex activation in the mouse. PLoS One *9*, e94657. 10.1371/journal.pone.0094657.
59. van Heukelum, S., Tulva, K., Geers, F.E., van Dulm, S., Ruisch, I.H., Mill, J., Viana, J.F., Beckmann, C.F., Buitelaar, J.K., Poelmans, G., et al. (2021). A central role for anterior cingulate cortex in the control of pathological aggression. Current Biology *31*, 2321-2333.e2325. https://doi.org/10.1016/j.cub.2021.03.062.
60. Soden, M.E., Yee, J.X., Cuevas, B., Rastani, A., Elum, J., and Zweifel, L.S. (2022). Distinct Encoding of Reward and Aversion by Peptidergic BNST Inputs to the VTA. Front Neural Circuits *16*, 918839. 10.3389/fncir.2022.918839.
61. Kim, D.I., Kang, S.J., Jhang, J., Jo, Y.S., Park, S., Ye, M., Pyeon, G.H., Im, G.H., Kim, S.G., and Han, S. (2024). Encoding opposing valences through frequency-dependent transmitter switching in single peptidergic neurons. bioRxiv. 10.1101/2024.11.09.622790.

62. Gerachshenko, T., Blackmer, T., Yoon, E.J., Bartleson, C., Hamm, H.E., and Alford, S. (2005). Gbetagamma acts at the C terminus of SNAP-25 to mediate presynaptic inhibition. Nat Neurosci *8*, 597-605. 10.1038/nn1439.
63. Roth, B.L. (2016). DREADDs for Neuroscientists. Neuron *89*, 683-694. 10.1016/j.neuron.2016.01.040.
64. Arora, S., Saarloos, I., Kooistra, R., Van De Bospoort, R., Verhage, M., and Toonen, R.F. (2017). SNAP-25 gene family members differentially support secretory vesicle fusion. Journal of Cell Science *130*, 1877-1889.
65. Abramian, A., Hoogstraaten, R.I., Murphy, F.H., McDaniel, K.F., Toonen, R.F., and Verhage, M. (2024). Rabphilin-3A negatively regulates neuropeptide release, through its SNAP25 interaction. Elife *13*. 10.7554/eLife.95371.
66. Siever, L.J. (2008). Neurobiology of aggression and violence. Am J Psychiatry *165*, 429-442. 10.1176/appi.ajp.2008.07111774.
67. Everitt, B.J., and Robbins, T.W. (2016). Drug Addiction: Updating Actions to Habits to Compulsions Ten Years On. Annu Rev Psychol *67*, 23-50. 10.1146/annurev-psych-122414-033457.
68. Cai, H., Haubensak, W., Anthony, T.E., and Anderson, D.J. (2014). Central amygdala PKC-δ+ neurons mediate the influence of multiple anorexigenic signals. Nature neuroscience *17*, 1240-1248.
69. Wu, Y.E., Pan, L., Zuo, Y., Li, X., and Hong, W. (2017). Detecting Activated Cell Populations Using Single-Cell RNA-Seq. Neuron *96*, 313-329.e316. 10.1016/j.neuron.2017.09.026.
70. Ayhan, F., Douglas, C., Lega, B.C., and Konopka, G. (2021). Nuclei isolation from surgically resected human hippocampus. STAR Protoc *2*, 100844. 10.1016/j.xpro.2021.100844.
71. Hao, Y., Hao, S., Andersen-Nissen, E., Mauck, W.M., 3rd, Zheng, S., Butler, A., Lee, M.J., Wilk, A.J., Darby, C., Zager, M., et al. (2021). Integrated analysis of multimodal single-cell data. Cell *184*, 3573-3587.e3529. 10.1016/j.cell.2021.04.048.
72. Bhattacherjee, A., Djekidel, M.N., Chen, R., Chen, W., Tuesta, L.M., and Zhang, Y. (2019). Cell type-specific transcriptional programs in mouse prefrontal cortex during adolescence and addiction. Nat Commun *10*, 4169. 10.1038/s41467-019-12054-3.

## FIGURES

**Figure 1. Social isolation alters social investigation and induces aggression in males and females. A**. Diagram showing experimental design of Resident Intruder (RI). **B-K** Males. **B**. Bar graph showing total duration (s) of face investigation towards intruder in group housed (GH) and isolated (SI) males, N=9 GH, 15 SI; Mann-Whitney test, $p < 0.05$ **C**. Bar graph showing total duration (s) of anogenital investigation towards intruder, N=9 GH, 15 SI, Mann-Whitney test $p > 0.05$. **D**. Bar graph showing total duration (s) of body investigation towards intruder, N=9 GH, 15 SI, Mann-Whitney test $p > 0.05$. **E.** Bar graph showing total duration (s) of aggression towards intruder in group housed (GH) and isolated (SI) males, N=9 GH, 15 SI; Mann-Whitney test, $p < 0.05$. **F**. Pie charts showing percent of total investigation directed towards body region (face, anogenital, or body). % Face GH v SI unpaired t-test, $p \leq 0.001$, Anogenital GH v SI unpaired t-test $p < 0.05$, Body GH v SI unpaired t-test, $p > 0.05$. N = 9 GH, 15 SI. **G**. Transition matrix showing probability of aggressive isolated males transitioning from one behavior to another, N=6. **H**. Diagram showing isolated males attack cycle. **I**. Raster plots showing behavioral sequence during RI assay in a group housed (GH) and isolated male (SI). **J**. Bar graph showing proportion of time engaged in anogenital investigation; GH: group housed male (N=15), pre-attack: isolated male before first attack, post attack: isolated males after first attack (N=7); One-way ANOVA, $p \leq 0.0001$, Tukey's multiple comparison's test: GH vs pre-attack $p < 0.01$, GH vs post attack $p > 0.05$, pre attack vs post attack $p < 0.0001$. **K**. Bar graph showing proportion of time engaged in body investigation; GH: group housed male (N=15), pre-attack: isolated male before first attack, post attack: isolated males after first attack (N=7); One-way ANOVA, $p < 0.01$, Tukey's multiple comparison's test: GH vs pre-attack $p > 0.05$, GH vs post attack $p > 0.05$, pre attack vs post attack $p < 0.01$. **L-U**. Females. **L**. Bar graph showing total duration (s) of face investigation towards intruder in group housed (GH) and isolated (SI) females, unpaired t-test $p \leq 0.001$, N = 13 GH, 16 SI. **M**. Bar graph showing total duration (s) of anogenital investigation towards intruder in group housed (GH) and isolated (SI) females, unpaired t-test $p < 0.001$. **N**. Bar graph showing total duration (s) of body investigation towards intruder in group housed (GH) and isolated (SI) females, unpaired t-test, $p < 0.0001$, N = 13 GH, 16 SI. **O**. Bar graph showing total duration (s) of aggression towards intruder in group housed (GH) and isolated (SI) females, Mann-Whitney test, $p < 0.05$. **P**. Pie charts showing percent of total investigation directed towards body region (face, anogenital, or body). % Face GH v SI Mann-Whitney test $p < 0.01$, Anogenital GH v SI unpaired t-test $p > 0.05$, Body GH v SI unpaired t-test, $p > 0.05$. N = 13 GH, 16 SI. **Q**. Transition matrix showing probability of aggressive SI females transitioning from one behavior to another, N = 10. **R**. Diagram showing isolated females transitioning between attack and body investigation. **S**. Raster plots showing behavioral sequence during RI assay in a group housed (GH) and isolated females (SI). **T**. Bar graph showing proportion of time engaged in anogenital investigation; GH: group housed female (N=13), pre-attack: isolated female before first attack, post attack: isolated females after first attack (N=10); One-way ANOVA, $p < 0.0001$, Tukey's multiple comparison's test: GH vs pre-attack $p < 0.0001$, GH vs post attack $p > 0.05$, pre attack vs post attack $p < 0.001$. **U**. Bar graph showing proportion of time engaged in body investigation; GH: group housed female (N=13), pre-attack: isolated female before first attack, post attack: isolated females after

first attack (N=10); One-way ANOVA $p < 0.01$, Tukey's multiple comparison's test: GH vs pre-attack $p > 0.05$, GH vs post attack $p > 0.05$, pre attack vs post attack $p < 0.01$. *Bars represent mean ± SEM. ns $p > 0.05$, * $p < 0.05$, ** $p < 0.01$, *** $p < 0.001$, **** $p < 0.0001$*

**Figure 2. Medial Prefrontal Cortex Tac2 neurons represent a small population of GABAergic neurons that are active during social encounters. A**. UMAP plot showing clustering of Tac2 neurons with other defined cortical cell types. **B**. Bar graph showing the proportion of excitatory and inhibitory neurons that express *Tac2*. **C**. Bar graph showing the proportion of Tac2 counts in cortical cell types. **D-G**. Representative images of RNAscope™ fluorescent in situ hybridization. scale bar represents 100µm. Tac2: Tachykinin-2, CRF: corticotropin releasing factor, SOM: somatostatin, PV: parvalbumin, VIP: Vasoactive intestinal peptide. **H**. Diagram showing prelimbic and infralimbic regions of medial prefrontal cortex with cortical layers. L1-3: layers 1-3, L5: layer 5, L6: layer 6. **I**. Pie chart showing percent of Tac2 cells expressing CRF (N=6 animals, 3 GH, 3 SI; 2 Male, ~ 3 sections/animal), SOM (N=4 animals, 2 GH, 2 SI; 1 Male, ~3 sections/animal), PV (N=6 animals, 3 GH, 3 SI; 4 Male, ~3 sections/animal), and VIP (N=8 animals (4 GH, 4 SI; 4M). **J**. Pie chart showing the percent of Tac2 cells in cortical layers. **K**. Pie chart showing the percent of Tac2 cells that percent VIP in early (L1-3) and deep (L5-6) cortical layers. **L**. Diagram showing prelimbic and infralimbic regions of medial prefrontal cortex with cortical layers. L1-3: layers 1-3, L5: layer 5, L6: layer 6. **M**. Representative image showing Tac2 cFos in situ hybridization across the cortical layers. Bar represents 100µm. **N**. Bar graph showing the percent of Tac2 cells expressing cFos in layers 1-3 (N = 4, 2 SI, 2 GH, 2 Males, ~ 3 sections/animal); nested t-test $p < 0.01$. **O**. Bar graph showing the percent of Tac2 cells expressing cFos in layer 5 (N = 4, 2 SI, 2 GH, 2 Males, ~3 sections/animal); nested t-test $p > 0.05$. **P**. Bar graph showing the percent of Tac2 cells expressing cFos in layer 6 (N = 4, 2 SI, 2 GH, 2 Males, ~3 sections/animal); nested t-test $p > 0.05$. **Q**. Diagram showing viral infusion into infralimbic mPFC. **R**. Representative image showing Tac2 neuron axons labeled with GFP and the cortical layers. **S**. Representative image showing Tac2 neuronal terminals (synaptophysin) in red (mRuby). **T**. Merged image showing axonal arbor (green) and terminals (red) of Tac2 neurons. **R-T** scale bar represents 100µm. *Bars are mean ± SEM ns $p > 0.05$, * $p < 0.05$, ** $p < 0.01$, *** $p < 0.001$*

**Figure 3. mPFC Tac2 neuron activity is required for isolation-induced aggression**
**A**. Proposed model of increased Tac2 neuronal activity isolated (SI) mice, compared to group housed (GH) mice, resulting in aggression and altered investigation behaviors. **B**. Experimental approach for DREADD-mediated inhibition of mPFC Tac2 neurons. **C**. Representative image of hM4Di-mCherry labeled Tac2 neurons in infralimbic mPFC, sale bar represents 100 µm. **D-G**. Bar graphs showing effects of DREADD-mediation inhibition of mPFC Tac2 neurons in mice given vehicle (VEH) or DCZ (Deschloroclozapine), bars are mean ± SEM; N = 8 M, 5 F. **D**. Face investigation: Wilcoxon test, $p>0.05$. **E**. Anogenital investigation: Wilcoxon test, $p>0.05$. **F**. Body investigation: Paired t-test, $p > 0.05$. **G**. Aggression: Wilcoxon test, $p<0.01$. *Bars represent mean ± SEM, * $p<0.05$ ** $p<0.01$*

**Figure 4. Knockdown of Tac2 in mPFC of isolated mice alters investigation, but not aggression. A**. Experimental approach for knockdown of Tac2 in mPFC and subsequent behavioral testing. **B**. Verification of Tac2 knockdown via RNAscope for Tac2 in mPFC. Nested t test, $p < 0.05$, N = 3 shLuc, 3 shTac2 (5M, 1 F, ~3 section/animal), scale bars represent 50µm. **C**. Bar graph showing total duration of face investigation in Luciferase shRNA mice (shLuc) and Tac2 shRNA mice (shTac2), Mann-Whitney test, $p > 0.05$. **D**. Bar graph showing total duration (s) of anogenital investigation in Luciferase shRNA mice (shLuc) and Tac2 shRNA mice (shTac2), unpaired t-test, $p < 0.1$. **E**. Bar graph showing total duration (s) of body investigation in Luciferase shRNA mice (shLuc) and Tac2 shRNA mice (shTac2), Mann-Whitney test, $p < 0.05$. **F**. Bar graph showing total duration of aggression in Luciferase shRNA mice (shLuc) and Tac2 shRNA mice (shTac2), Mann-Whitney test, $p > 0.05$. *Bars represent mean ± SEM, individual dots represent mean duration for each animal, ns $p > 0.05$, * $p < 0.05$*

**Figure 5. GABA release from mPFC Tac2 neurons controls isolation-induced aggression A**. Experimental workflow to infuse CRISPR viruses into mPFC of Tac2-Cre mice. **B**. Representative image of EGFP-KASH to visualize viral infusion site bar represents 100 µm. **C**. Bar graph showing total duration (s) of face investigation in mice with guide RNA directed to the Rosa26 locus (sgRosa26) or Slc32a1 (sgSlc32a1), Mann-Whitney test, $p > 0.05$. s **D**. Bar graph showing total duration (s) of body investigation in mice with guide RNA directed to the Rosa26 locus (sgRosa26) or Slc32a1 (sgSlc32a1), unpaired t-test, $p > 0.05$. **E**. Bar graph showing total duration (s) of body investigation in mice with guide RNA directed to the Rosa26 locus (sgRosa26) or Slc32a1 (sgSlc32a1), unpaired t- test, $p > 0.05$. **F**. Bar graph showing total duration (s) of aggression in mice with guide RNA directed to the Rosa26 locus (sgRosa26) or Slc32a1 (sgSlc32a1), Mann-Whitney test, $p < 0.01$. **G**. Proposed model of neurokinin B and GABA release from mPFC Tac2 neurons to control distinct isolation-induced behaviors (investigation and aggression). *Bar represent mean ± SEM, Lighter dots on bars represent mean of individual female, darker dots males male; ns $p > 0.05$, * $p < 0.05$, ** $p < 0.01$, *** $p < 0.001$*

**Figure 6. mPFC Neurokinin-3 receptor neurons are impacted by social isolation in a cell type specific manner**. **A**. Diagram of prelimbic (PrL) and infralimbic (IL) regions of medial prefrontal cortex and cortical layers within each. Representative image of cFos and Tacr3/Nk3R in situ hybridization. Scale bar represents 50µm. **B**. Bar graph showing the percent of Tacr3/Nk3R cells expressing cFos in group housed (GH) and isolated (SI) mice; N = 4 animals, 2 GH, 2 SI, 4 F, ~3 sections/animal. **C**. Bar graph showing percent of Tacr3/Nk3R cells expressing cFos in layers 1-3; N = 2 animals, 1 GH, 1 SI, 2 F, ~3 sections/animal; unpaired t-test $p < 0.1$. **D**. Bar graph showing percent of Tacr3/Nk3R cells expressing cFos in layer 5; N = 2 animals, 1 GH, 1 SI, 2 F, ~3 sections/animal; unpaired t-test, $p > 0.05$. **E**. Bar graph showing percent of Tacr3/Nk3R cells expressing cFos in layer 6; N = 2 animals, 1 GH, 1 SI, 2 F, ~3 sections/animal; unpaired t-test $p < 0.05$. **F**. UMAP plot showing Nk3R cells clustering with known mPFC cell types. **G**. Bar graph showing the proportion of Tacr3/Nk3R counts from excitatory and inhibitory neurons, N = 3 males per housing condition, one-way ANOVA, Housing x cell type interaction $p < 0.01$, main effect cell type $p < 0.001$, Sidak's multiple comparisons test GH v SI inhibitory $p < 0.05$. **H**. Bar graph showing the proportion of Tacr3/Nk3R counts in group housed (GH) and isolated (SI) males (N = 3 animals per housing condition); two-way ANOVA cell type x housing interaction $p < 0.05$, main effect cell type $p < 0.01$, uncorrected Fisher's LSD: GH vs SI L2/3 Exc (L2/3 Exc) $p < 0.05$, L6 Exc (layer 6 excitatory), $p < 0.1$, L6b CTX (layer 6b of cortex) $p < 0.05$, SOM (somatostatin neurons) $p < 0.1$. **I**. Experimental workflow of DREADD-mediated activation of Tacr3/Nk3R neurons. **J**. Representative image showing Tacr3/Nk3R neurons (red); scale bar represents 100µm. **K**. Bar graph showing total duration of face investigation in animals on vehicle (VEH) and DCZ (Deschloroclozapine), Wilcoxon test $p > 0.05$. **L**. Bar graph total duration of anogenital investigation in animals on vehicle (VEH) and DCZ (Deschloroclozapine), Wilcoxon test $p > 0.05$. **M**. Bar graph showing total duration of body investigation in animals on vehicle (VEH) and DCZ (Deschloroclozapine), paired t-test $p > 0.05$. **N**. Bar graph showing total duration of aggression in animals on vehicle (VEH) and DCZ (Deschloroclozapine), Wilcoxon test $p > 0.05$. **K-N**. N = 9 animals (7 M, 3 F); darker color dots on bars represent males, lighter dots present females. *All bars show mean ± SEM, ns $p > 0.05$, * $p < 0.05$*

**Supplemental Figure 1. Face investigation remains unchanged in SI animals post attack. A**. Bar graph showing the proportion of time group housed (GH) males and isolated males (pre and post attack) engage in face investigation (N = 9 GH, 7 SI); one-way ANOVA $p < 0.05$, Tukey's multiple comparions test: GH vs pre attack $p < 0.05$, GH vs post attack $p > 0.05$, pre attack vs post attack $p < 0.1$. **B**. Bar graph showing the proportion of time group housed (GH) and isolated females (pre and post attack) engage in face investigation (N= 13 GH, 10 SI); one-way ANOVA $p > 0.05$. *Bars represent mean ± SEM, ns p > 0.05 * p< 0,05.*

**Supplemental Figure 2. Characterization and activity profile of mPFC Tac2 cells during Resident Intruder assay. A**. Representative image of in situ hybridization for Tac2 and GAD1/2 in infralimbic mPFC; scale bar represents 100µm. **B**. Representative image of in situ hybridization for Tac2 and Slca717 in infralimbic mPFC; scale bar represents 100µm. **C**. Pie chart showing Tac2 expression within GAD1/2-positive cells and Slca717-positive cells; N = 2 males (1 GH, 1 SI, ~ 3 sections per animal) for both GAD1/2 and Slca717 staining. **D**. Proportion of Tac2 counts from sn-RNAseq in various cell types (N = 3 males per housing condition). **E**. Percent of total Tac2 cells expressing cFos in mPFC from group housed GH) and isolated (SI) mice (N = 4 animals, 2 per housing condition, 2 F, 2 M per housing condition); nested t-test, $p < 0.1$. **F**. Representative image of in situ hybridization across cortical layers for Tac2, cFos, and VIP scale bar represents 100µm. **G-P**. N = 2 females, 1 GH, 1 SI. **G**. Bar graph showing percent of all Tac2 cells in mPFC expressing both cFos and VIP, Mann-Whitney test, $p > 0.05$. **H**. Bar graph showing percent of Tac2 cells in layers 1-3 expressing both cFos and VIP, Mann-Whitney test, $p > 0.05$. **I**. Bar graph showing percent of Tac2 cells in layer 5 expressing both cFos and VIP, Mann-Whitney test, $p > 0.05$. **J**. Bar graph showing percent of Tac2 cells in layer 6 expressing both cFos and VIP, Mann-Whitney test, $p > 0.05$. **L**. Bar graph showing percent of total VIP cells expressing cFos in mPFC, Mann-Whitney test, $p > 0.05$. **M**. Bar graph showing percent of VIP cells in layers 1-3 expressing cFos, Mann-Whitney test, $p > 0.05$. **N**. Bar graph showing percent t of VIP cells in layer 5 expressing cFos, Mann-Whitney test, $p > 0.05$. **O**. Bar graph showing percent of VIP cells in layer 6 expressing cFos, Mann-Whitney test, $p > 0.05$. **P**. Bar graph showing percent of total Tac2 cells that express cFos, but not VIP, Mann-Whitney test $p > 0.05$.

**Supplemental Figure 3. Dose-response relationship between DCZ and behavior in the Resident Intruder Assay.** Dots with connecting line show mean duration of behavior for each animal. Darker colors represent males, light colors females. **A-F**. 0.1 mg/kg DCZ. **A**. Graph showing total duration of face investigation when isolated animals received vehicle (VEH) and 0.1 mg/kg Deschloroclozapine (DCZ), N = 7 F, 7 M; Wilcoxon test, $p > 0.05$. **B**. Same as A but showing total duration of anogenital investigation; Wilcoxon test, $p > 0.05$. **C**. Same as A but showing total duration of body investigation; Wilcoxon test, $p > 0.05$. **D**. Same as A, but showing total duration of aggression; Wilcoxon test, $p > 0.05$. **E**. Workflow of cFos immunohistochemistry on animals expressing hM4D in mPFC Tac2 neurons. **F**. Bar graph showing reduction in the percent of cells expressing cFos in mice on vehicle (VEH) and Deschloroclozapine (DCZ), Nested t-test $p < 0.05$, N = 3 DCZ, 3 VEH, ~ 4 sections per animal, 2 M, 1 F per drug condition; bars represent mean ± SEM **G-J**. 0.25 mg/kg DCZ. **G**. Graph showing total duration of face investigation when isolated animals received vehicle (VEH) and 0.25mg/kg Deschloroclozapine (DCZ); N = 4 M, 3 F, Wilcoxon test, $p > 0.05$; **H**. Same as G, but showing total duration of anogenital investigation; Wilcoxon test, $p > 0.05$. **I**. Same as G, but total duration of body investigation; paired t-test, $p > 0.05$. **J**. Same as G but showing total duration of aggression; Wilcoxon test $p > 0.05$. **K-N**. 0.5 mg/kg DCZ. **K**. Graph showing total duration of face investigation when isolated animals received vehicle (VEH) or 0.5 mg/kg Deschloroclozapine (DCZ), N = 8 M, 7 F; Wilcoxon test $p < 0.001$. **L** Same as K, but showing total duration of anogenital investigation, Wilcoxon test, $p > 0.05$. **M**. Same as K, but showing total duration of body investigation, Wilcoxon test, $p < 0.1$. **N**. Same as K, but showing total duration of aggression, Wilcoxon test, $p < 0.05$. **O-R**. 1.0 mg/kg DCZ. **O**. Graph showing total duration of face investigation when isolated animals received vehicle (VEH) and 1.0 mg/kg Deschloroclozapine (DCZ), N = 3 F, 6 M; Wilcoxon test, $p < 0.1$. **P**. Same as O, but showing total duration of anogenital investigation, Wilcoxon test, $p > 0.05$. **Q**. Same as O, but showing total duration of body investigation, Wilcoxon test, $p > 0.05$. **R**. Same as O, but showing total duration of aggression, Wilcoxon test, $p > 0.05$.

**Supplemental Figure 4. DREADD-mediated inhibition of mPFC Tac2 neurons reduces aggression in both sexes**. **A-E**. Males. **A**. Bar graph showing total duration of face investigation isolated males expressing hM4D in mPFC Tac2 neurons, N = 8, paired t-test, $p > 0.05$. **B**. Same as a A, but showing total duration of anogenital investigation, Wilcoxon test, $p > 0.05$. **C**. Same as A, but showing total duration of body investigation, paired t-test, $p > 0.05$. **D**. Same as A, but showing total duration of aggression, Wilcoxon test, $p < 0.5$. **E-H**. Females. **E**. Bar graph showing total duration of face investigation in isolated females expressing hM4D in mPFC Tac2 neurons, N = 5, Wilcoxon test, $p > 0.05$. **F**. Same as E, but showing total duration of anogenital investigation, paired t-test, $p > 0.05$. **G**. Same as E, but showing the total duration of body investigation, paired t-test, $p > 0.05$. **H**. Same as E, but showing the total duration of aggression, Wilcoxon test, $p < 0.1$. *Bars represent mean ± SEM, individual dots with connecting lines show mean duration of behavior for each animal on each drug. ns $p > 0.05$, * $p < 0.05$*

**Supplemental figure 5. Knockdown of Tac2 in mPFC impacts distinct isolation induced investigation behaviors in male and females. A-D.** Males, N = 12 shLuc, 7 shTac2. **A**. Graph showing total duration of aggression in isolated males with the shRNA shLuciferase (shLuc) or the shTac2 in the mPFC, Mann-Whitney test, $p > 0.05$. **B**. Same as A, but graph shows total duration of face investigation, Mann-Whitney test, $p > 0.05$. **C**. Same as A, but graph shows total duration of anogenital investigation, unpaired t-test, $p > 0.05$. **D**. Same as A, but graph shows total duration of body investigation, unpaired t-test, $p < 0.1$. **E-H**. Females, N = 15 shLuc, 11 shTac2. **E**. Graph showing the total duration of body investigation in shLuc and shTac2 isolated females, Mann-Whitney test, $p > 0.05$. **F**. Same as E, but showing total duration of face investigation, Mann-Whitney test, $p > 0.05$. **G**. Same as E, but showing total duration of anogenital investigation, Mann-Whitney test, $p < 0.1$. **H**. Same as E, but showing the total duration of body investigation, Mann-Whitney test, $p > 0.05$. *Bars represent mean ± SEM, individual dots represent mean of individual animals; ns $p > 0.05$, * $p < 0.05$*

**Supplemental Figure 6. Sex-independent effects of *Slc32a1* missense mutations in mPFC Tac2 neurons of isolated mice. A-B.** Males; N = 7 sgRosa26, 9 sgSLC32a1. **A**. Graph showing total duration of aggression in isolated males with CRISPR/SaCas9 virus directed to the Rosa26 locus (sgRosa26) or to Slc32a1 (sgSlc32a1); Mann-Whitney test, $p < 0.05$. **B**. Same as A, but showing the total duration of face investigation, unpaired t-test, $p > 0.05$. **C**. Same as A, but showing the total duration of anogenital investigation, Mann-Whitney test, $p > 0.05$. **D**. Same as A, but showing the total duration of body investigation, unpaired t-test, $p > 0.05$. **E-F**. Females, N = 10 sgRosa26, 7 sgSlc32a1. **E**. Graph showing the total duration of aggression in isolated females with CRISPR/SaCas9 virus directed to the Rosa26 locus (sgRosa26) or to Slc32a1 (sgSlc32a1), Mann-Whitney test, $p < 0.05$. **F**. Same as E, but showing the total duration of face investigation, Mann-Whitney test $p > 0.05$. **G**. Same as E, but showing the total duration of anogenital investigation, unpaired t-test $p > 0.05$. **H**. Same as E, but showing the total duration of body investigation, unpaired t-test, $p > 0.05$. **I**. Graph showing the fluorescence intensity (mean grey value) of Slc32a1 fluorescently labeled mRNA in a mask of Tac2 cells from in situ hybridization, N = 1 F per viral condition, ~ 4 sections per animal, unpaired t-test $p < 0.001$. *Bars are mean ± SEM, individual dots in A-H represent mean duration for an individual animal. Dots in I represent mean grey value in the one hemisphere of infralimbic cortex of each section. Ns $p > 0.05$, * $p < 0.05$, ** $p < 0.01$, *** $p < 0.001$*

**Supplemental Figure 7: mPFC Tacr3/Nk3R cells are genetically tractable and distinct from mPFC Tac2 neurons. A**. Graph showing the proportion of distinct mPFC cell types in group housed (GH) and isolated (SI) animals that express Tacr3/Nk3R two-way ANOVA, cell type by housing interaction $p < 0.1$, uncorrected Fisher's LSD: SI L6 Car3, GH vs $p < 0.05$, SOM GH vs SI $p < 0.0001$. **B**. Proportion of Tacr3/Nk3R cells expression Tac2 in mPFC unpaired t-test, $p > 0.05$. **C**. Diagram showing experimental approach for confirmation of DREADD-mediated activation of Nk3R neurons through immunohistochemistry for cFos. **D**. Graph showing percent of cFos-positive cells in the mPFC of mice on vehicle (VEH) or Deschloroclozapine (DCZ), N = 3 M (2 VEH, 1 DCZ), 1 F, (1 VEH), ~3 sections per animal, unpaired t-test, $p < 0.05$. *Bars represent mean ± SEM, individual dots represent means for each animal, ns $p > 0.05$, * $p < 0.05$, ** $p < 0.01$, *** $p < 0.001$.*

# Figure 1: Social isolation alters social investigation and induces aggression in males and females

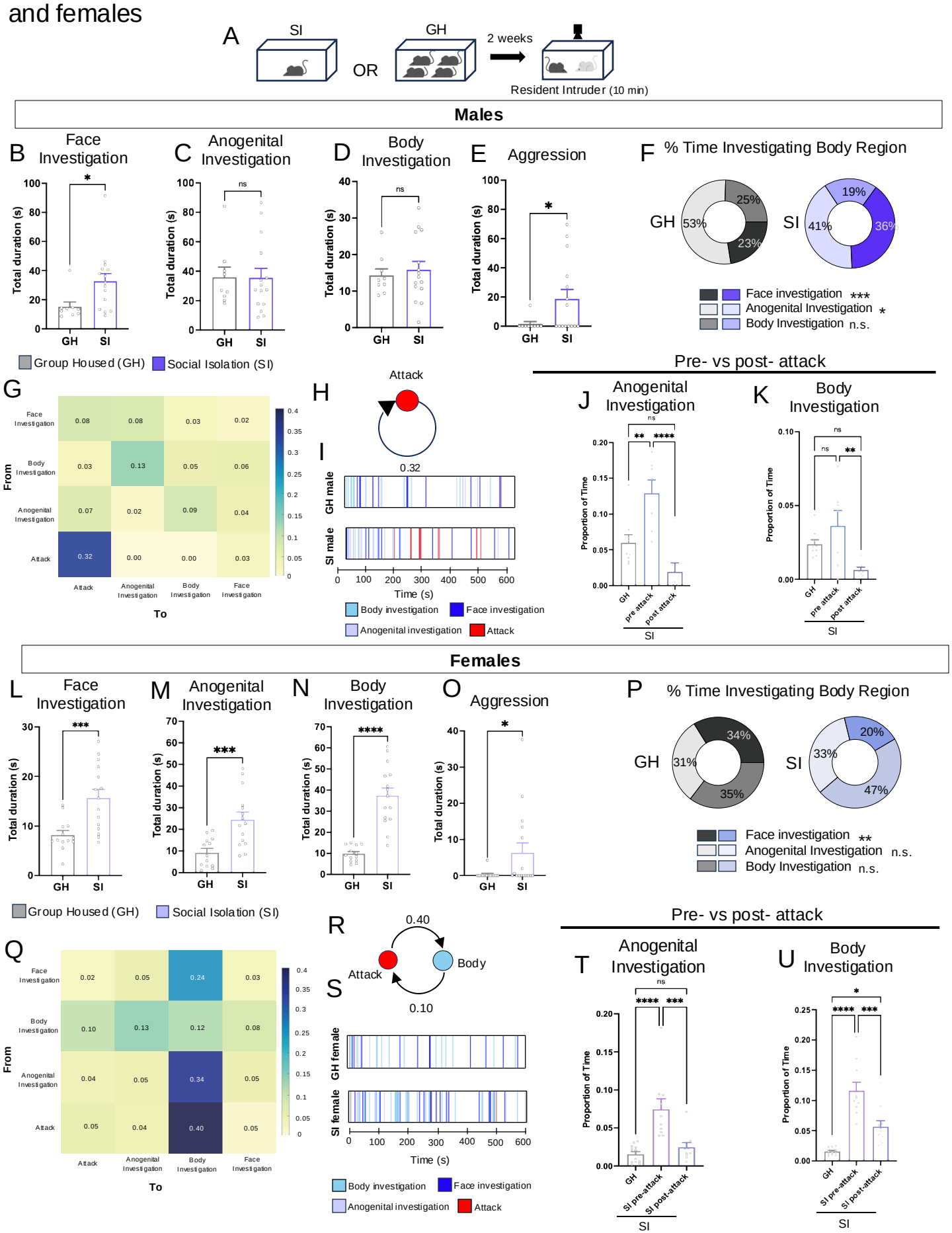

# Figure 2. Prefrontal Cortex Tac2 neurons represent a small population of GABAergic neurons that are active during social encounters

sn-RNAseq

A

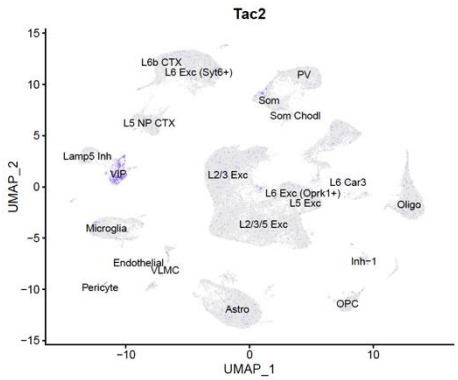


B

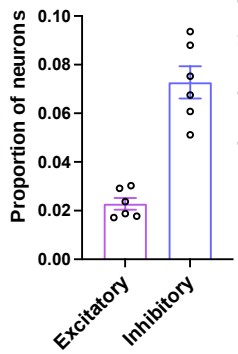


C

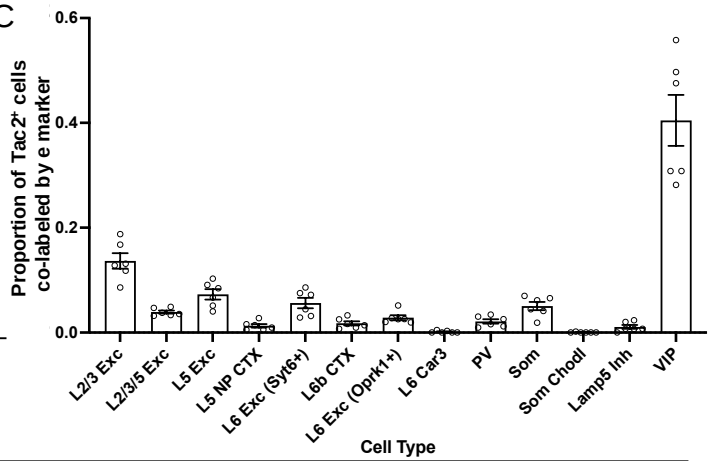


Fluorescent in situ hybridization highlights spatial and cell type distribution of Tac2 neurons in mPFC

D

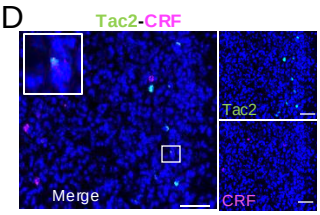


E

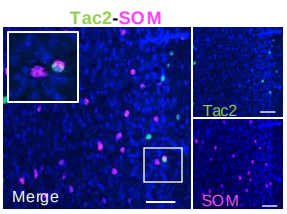


F

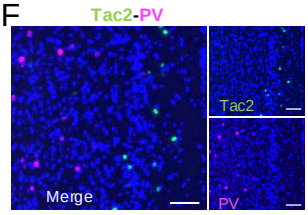


G

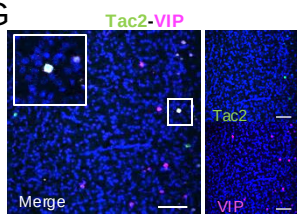


H

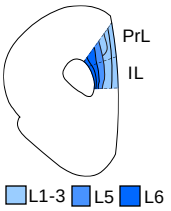


I

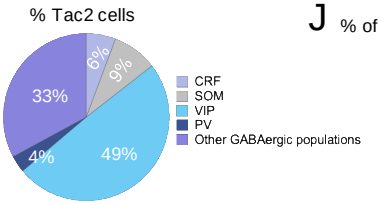


J

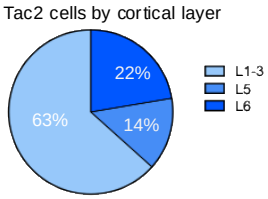


K

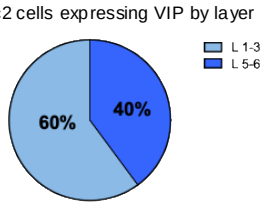


Tac2 neurons are differentially active in group housed and socially isolated mice

L

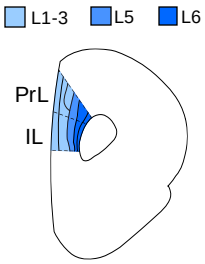


M

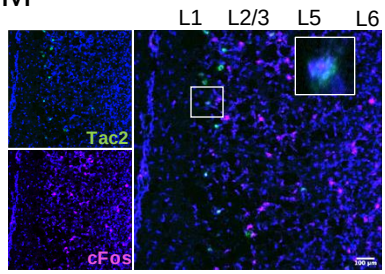


N

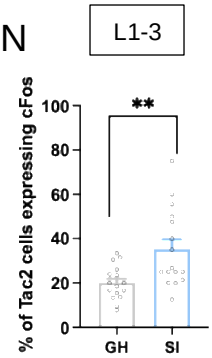


O

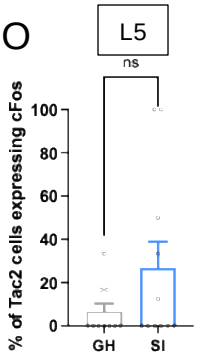


P

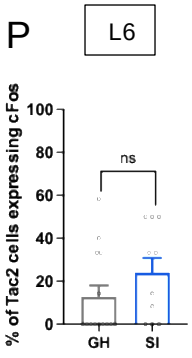


Axonal arbor and terminal distribution of mPFC Tac2 neurons

AAV2-hSyn-FLEx-mGFP-2A-Synaptophysin-mRuby

Q

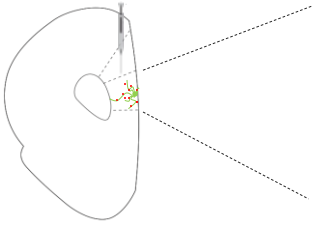


R

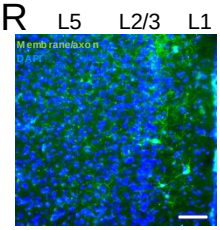


S

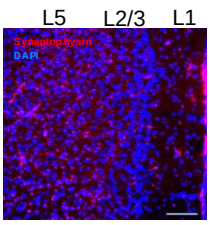


T

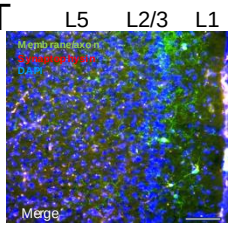

# Figure 3. mPFC Tac2 neuron activity is required for isolation-induced aggression

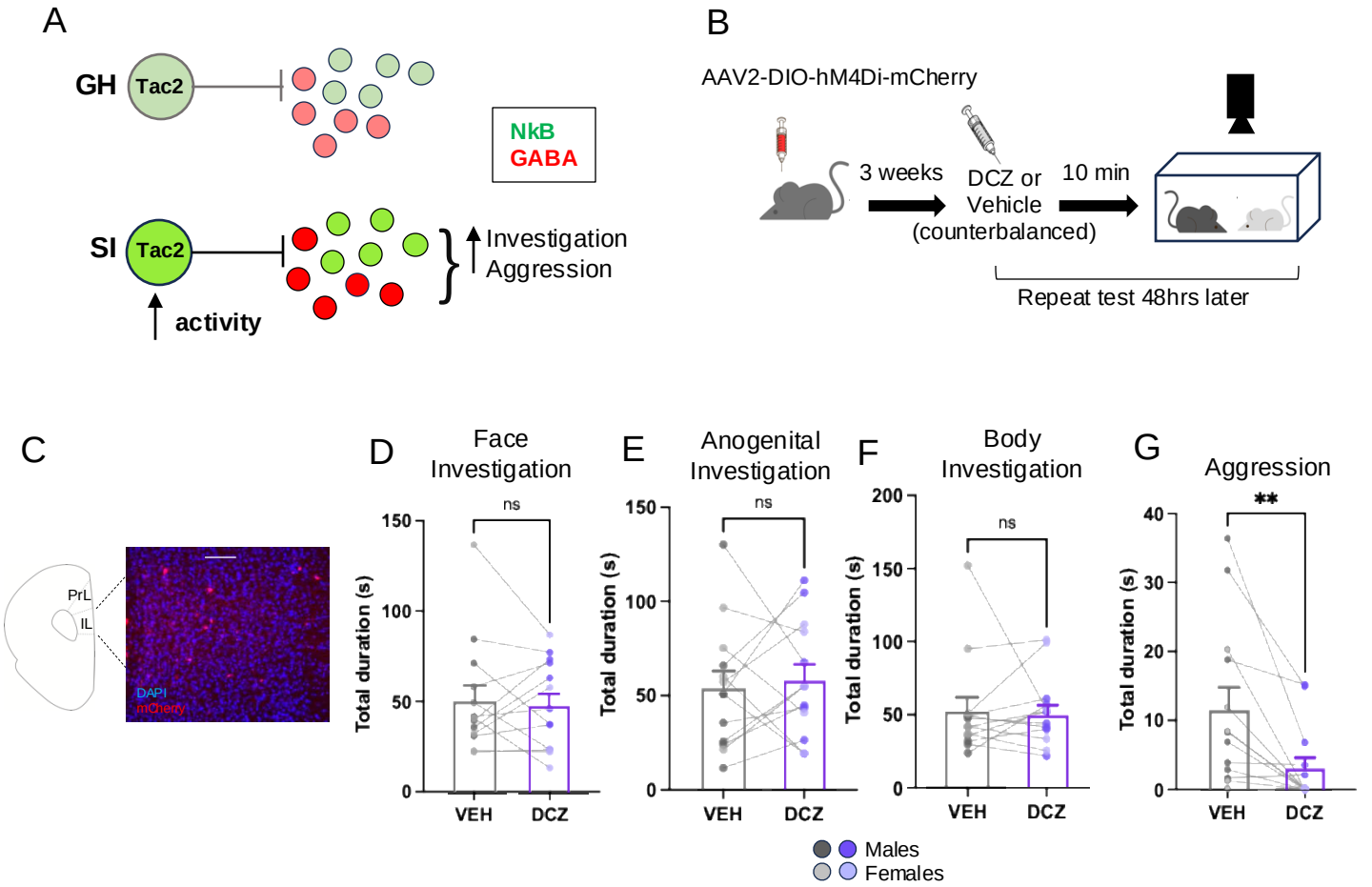

# Figure 4. Tac2 knockdown in mPFC of isolated alters investigation, but not aggression

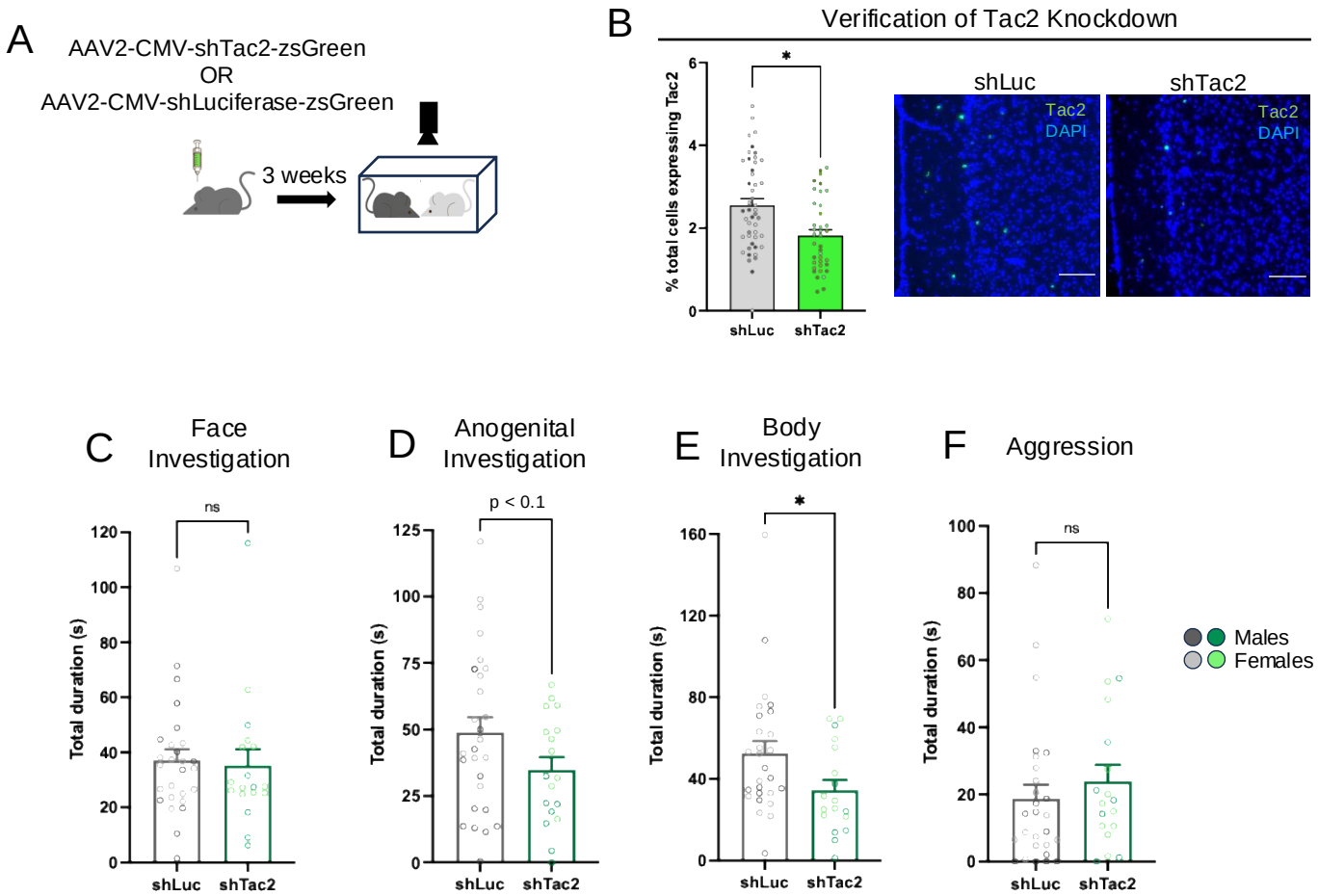

# Figure 5. GABA release from Tac2 neurons controls isolation induced aggression

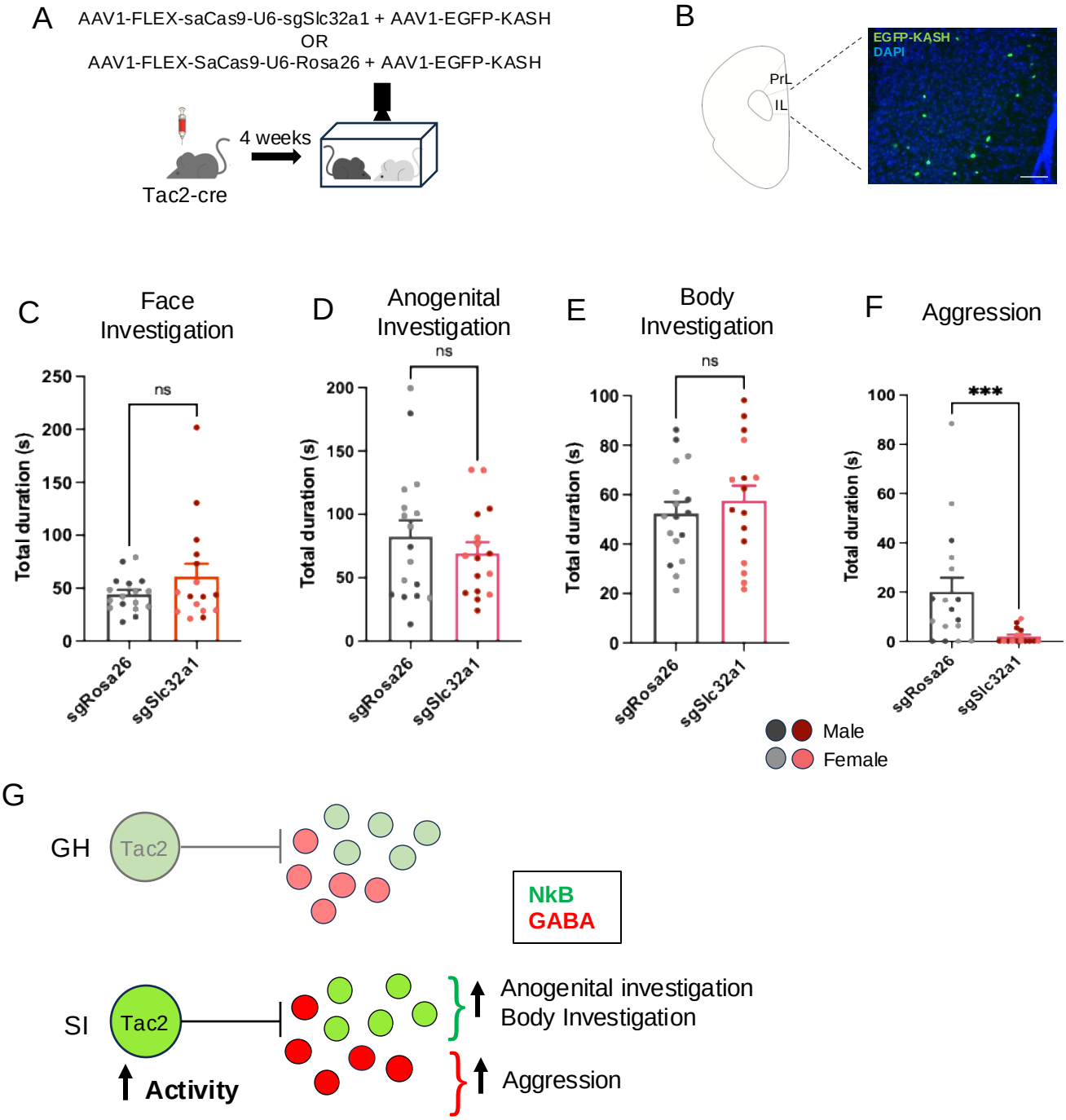

# Figure 6. mPFC Neurokinin-3 receptor neurons are impacted by social isolation in a cell-type specific manner

## Nk3R cells are differentially active during social encounters

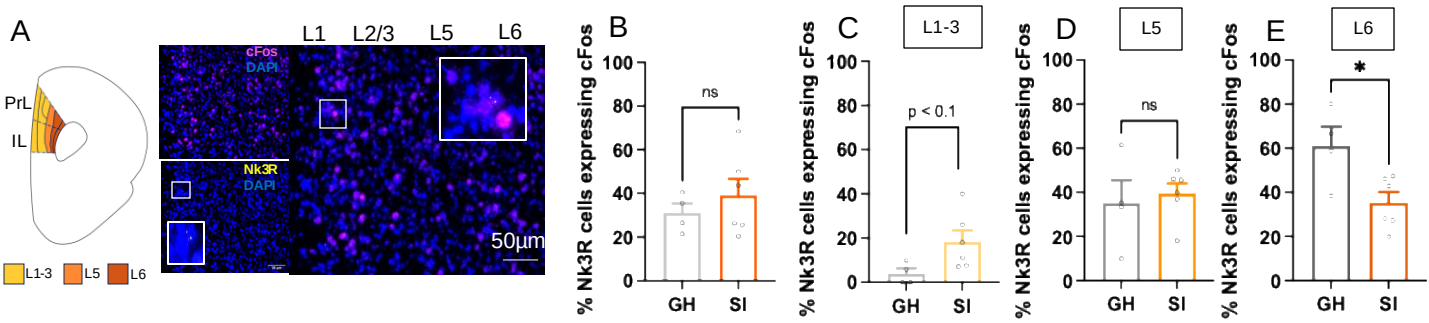


## Nk3R cells represent a diverse population that are impacted by isolation in a cell-type specific manner

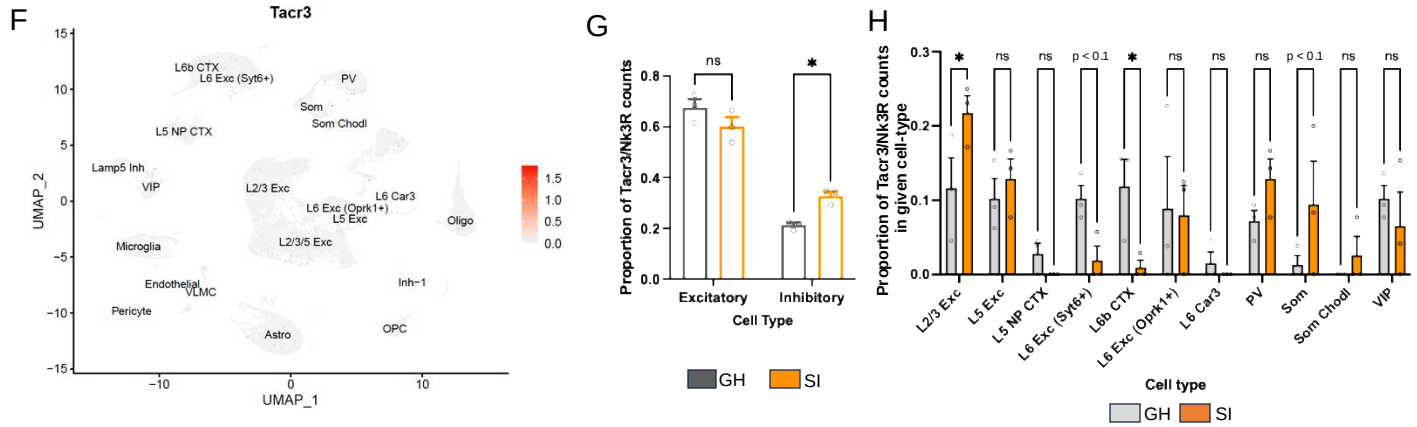


## DREADD-mediated manipulation of PFC Nk3R neuron activity

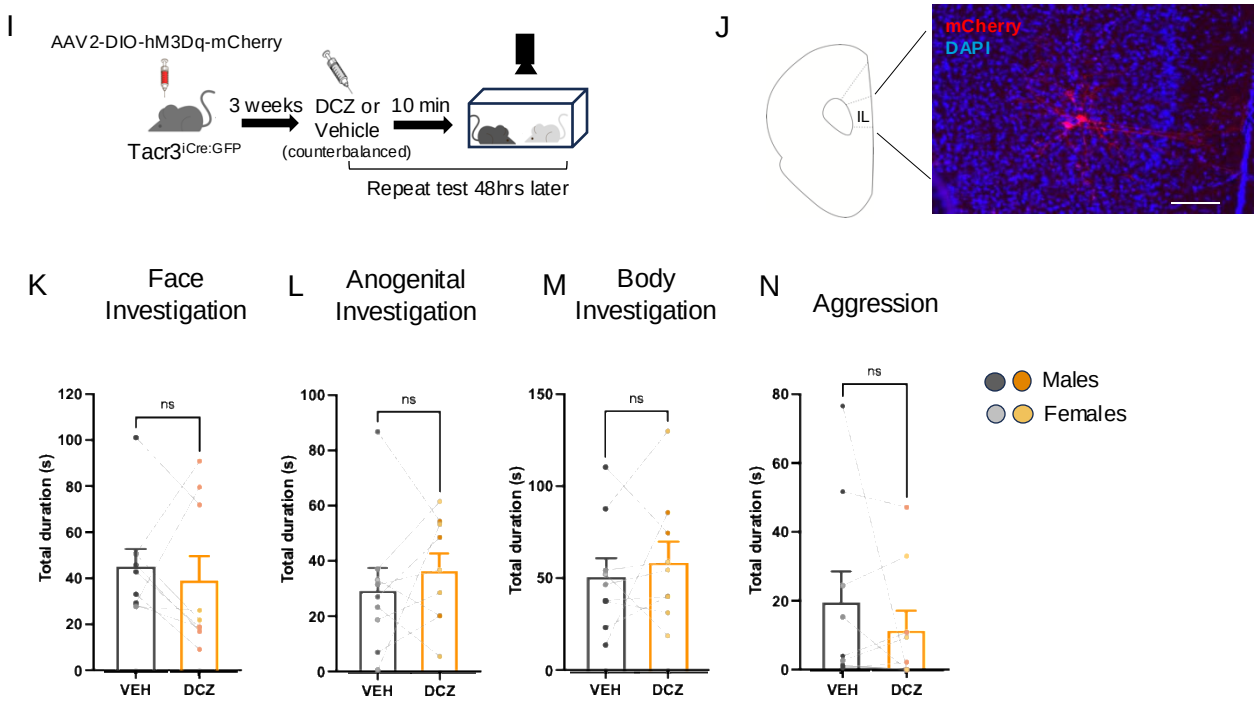

Supplemental Figure 1: Face investigation remains unchanged in SI animals post attack

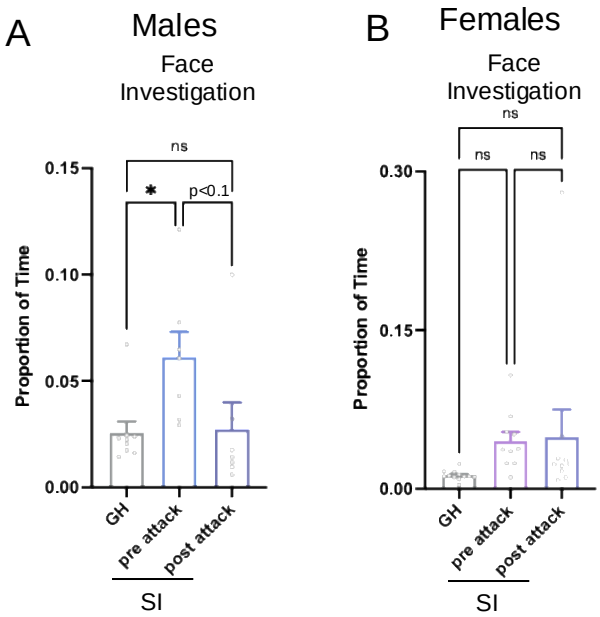

Supplemental Figure 2. Characterization and activity profile of Tac2 cells during Resident Intruder

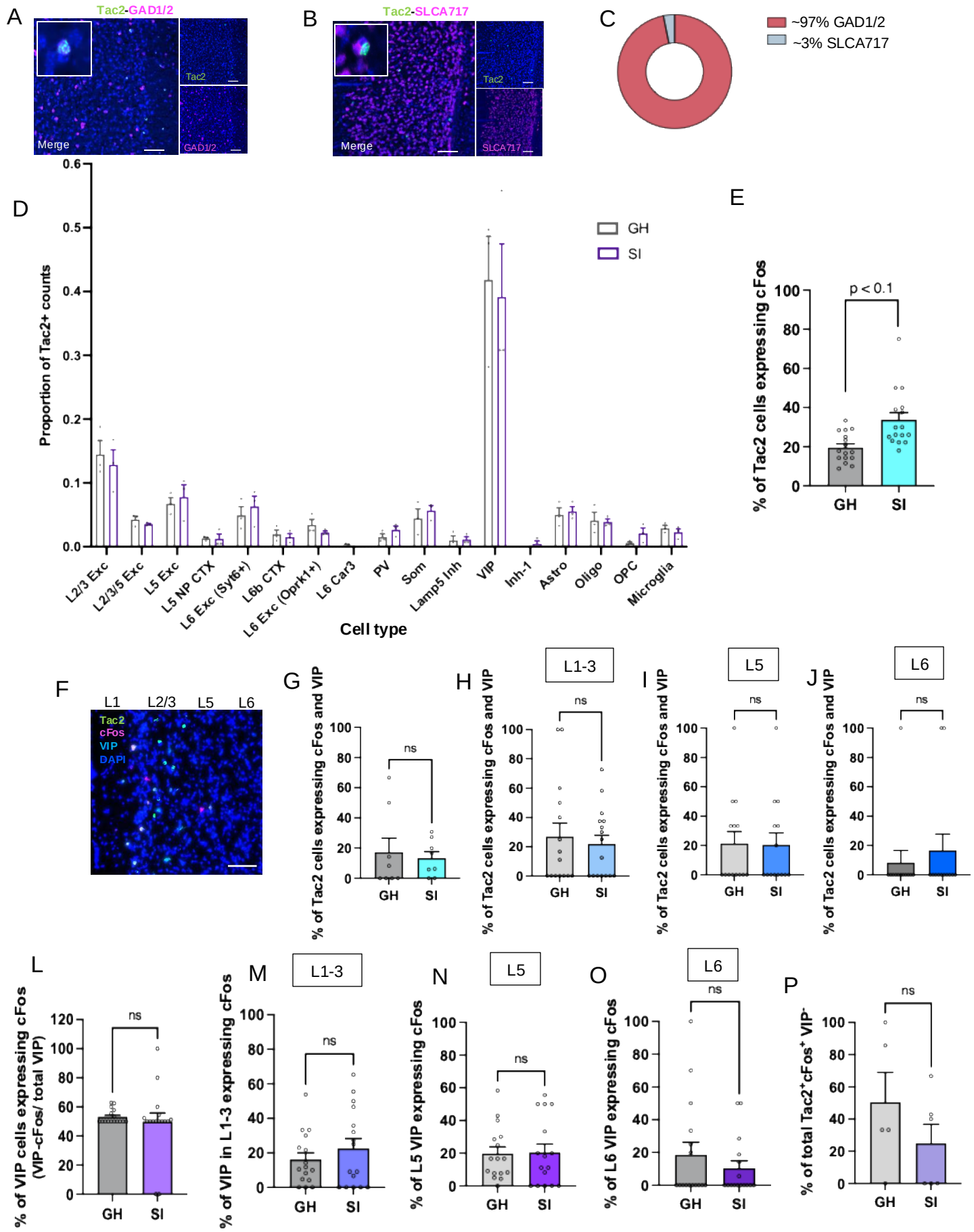

Supplemental Figure 3. Dose-response relationship between DCZ and behavior on the Resident Intruder Assay

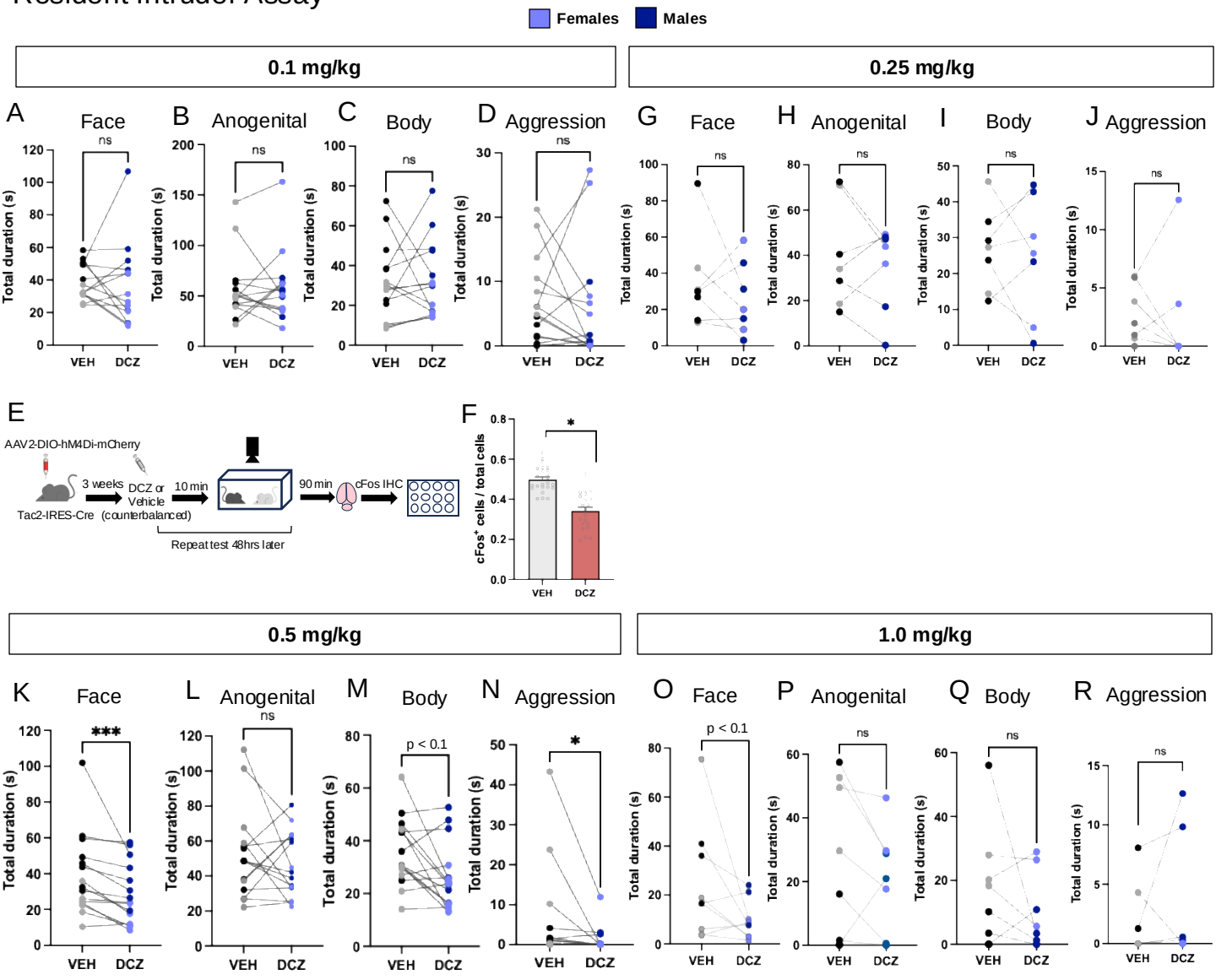

Supplemental Figure 4. DREADD-mediated inhibition of mPFC Tac2 neurons reduces aggression in sexes.

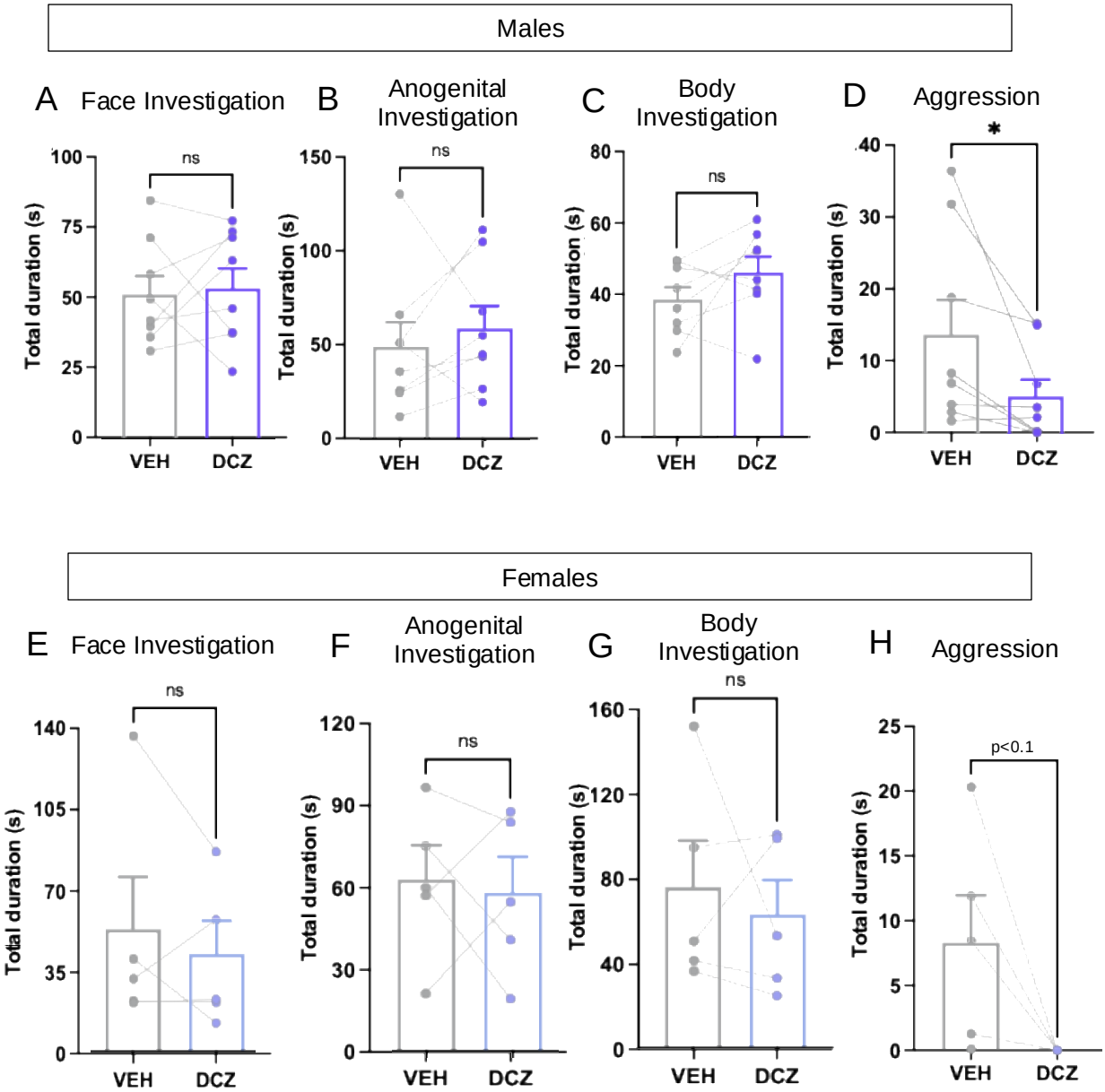

Supplemental Figure 5: Knockdown of Tac2 in mPFC impacts distinct isolation-induced investigation behaviors in males and females

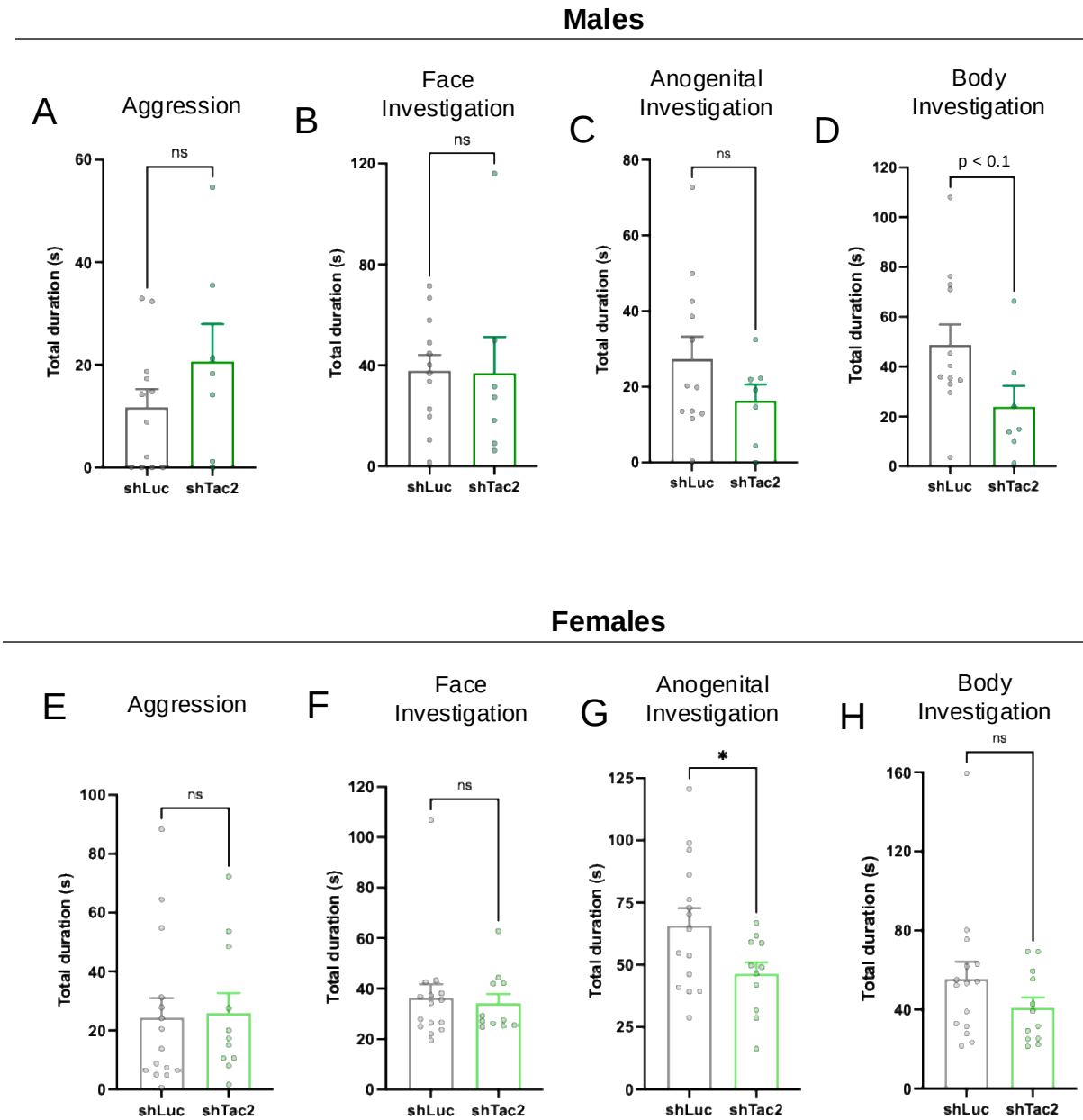

Supplemental figure 6: Sex-independent effects of Slc32a1 missense mutations in mPFC Tac2 neurons of isolated mice

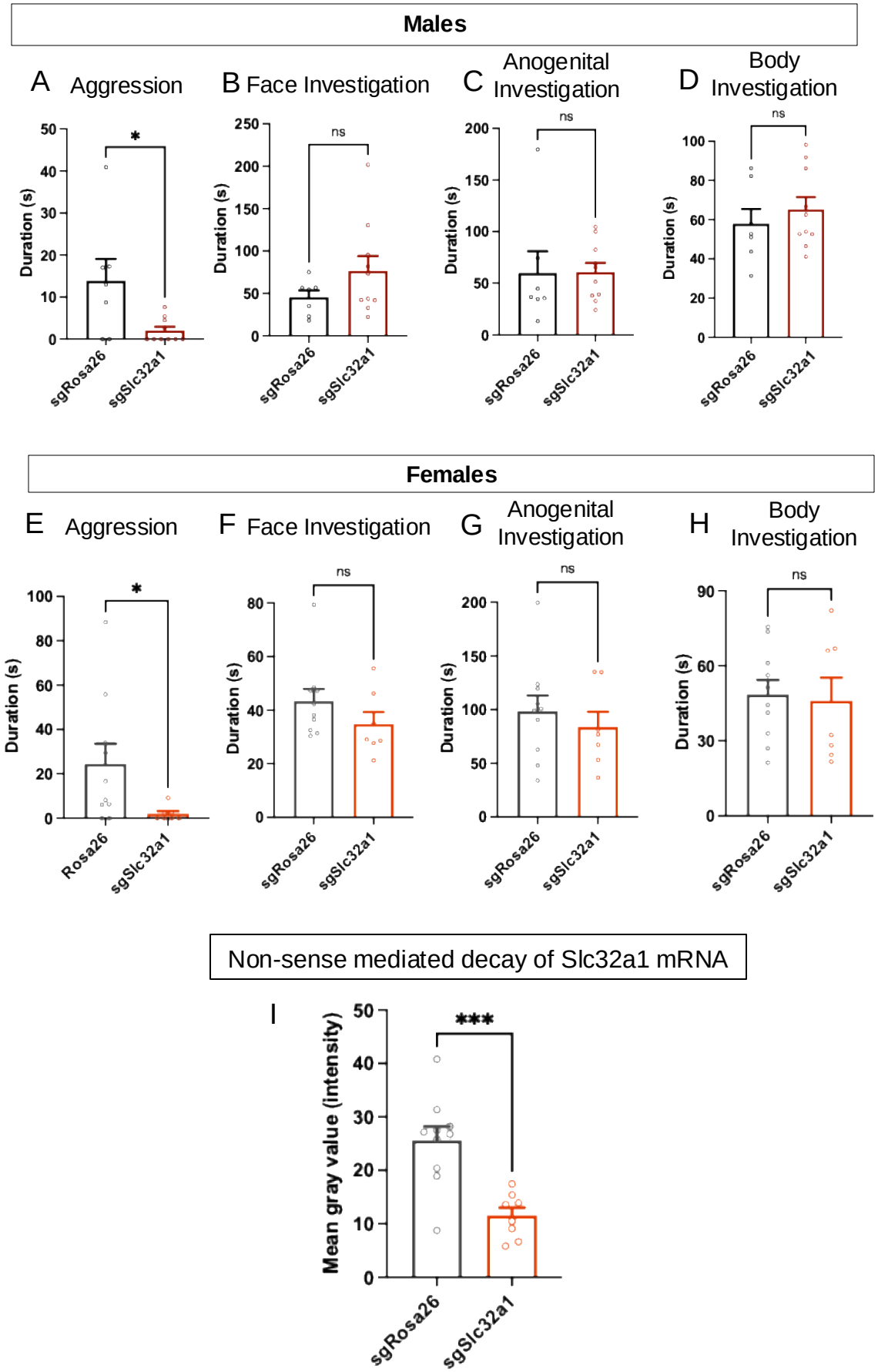

# Supplemental Figure 7: mPFC Tacr3/Nk3R cells are genetically-tractable and distinct from mPFC Tac2 neurons

A

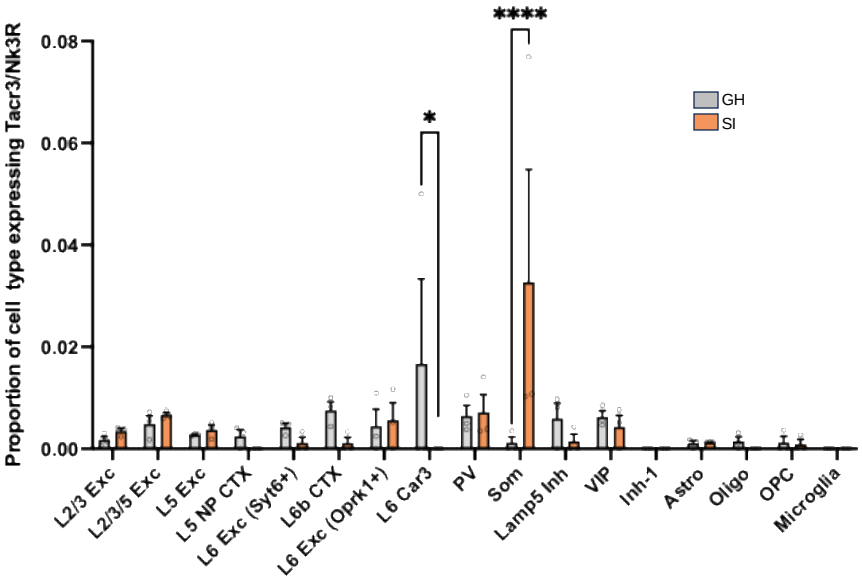


B

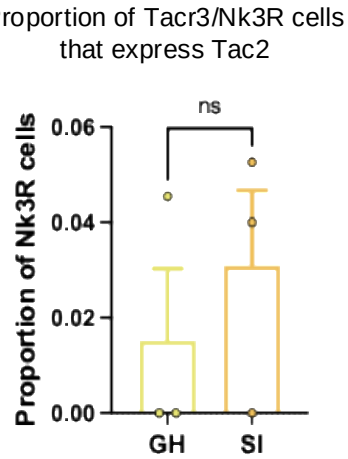


C

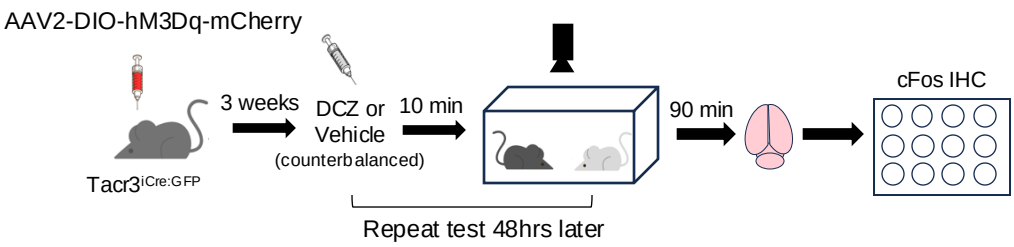

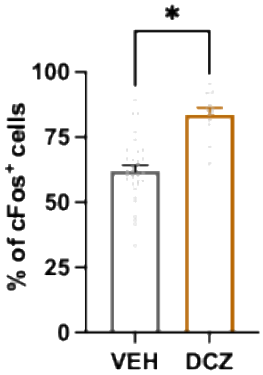
D